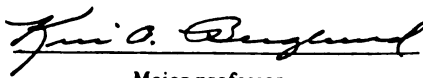




This is to certify that the
thesis entitled
Development of a Catalytic Process for the
Production of Maleic Anhydride from a Fermentation Feedstock

presented by
Sanjay Krishnamurthy Yedur

has been accepted towards fulfillment
of the requirements for
M. S. degree in Chem. Engr.


Major professor

Date June 17, 1992

LIBRARY
Michigan State
University

PLACE IN RETURN BOX to remove this checkout from your record.
TO AVOID FINES return on or before date due.

DATE DUE	DATE DUE	DATE DUE
NOV 13 1997 127033665		

MSU is An Affirmative Action/Equal Opportunity Institution

c:\crl\date\due.pm3-p.1

702-5026

**DEVELOPMENT OF A CATALYTIC PROCESS FOR THE
PRODUCTION OF MALEIC ANHYDRIDE FROM A
FERMENTATION FEEDSTOCK**

By

Sanjay Krishnamurthy Yedur

A THESIS

**Submitted to
Michigan State University
in partial fulfillment of the requirements
for the degree of
MASTER OF SCIENCE**

Department of Chemical Engineering

1992

ABSTRACT

DEVELOPMENT OF A CATALYTIC PROCESS FOR THE PRODUCTION OF MALEIC ANHYDRIDE FROM A FERMENTATION FEEDSTOCK

By

Sanjay Krishnamurthy Yedur

To reduce our dependency on non-renewable energy sources, it is necessary to develop alternate pathways for the production of various chemicals which are traditionally produced from feedstocks derived from fossil fuels. With this aim in view, an alternate process has been proposed for the production of maleic anhydride from a fermentation feedstock. The process utilizes the catalytic oxydehydrogenation of fermentation derived succinic anhydride to produce maleic anhydride. Various catalysts were synthesized and tested for the oxydehydrogenation reaction. Iron phosphate based catalysts were found to be the best on the basis of high conversions and selectivities obtained using these catalysts. The effect of temperature, oxygen concentration, feed concentration, contact time, and the total time on-stream on the performance of the catalyst was studied. A set of optimum conditions for the operation of the reactor was developed. The catalysts were characterized based on their bulk and surface compositions, their surface areas, and their bulk crystallographic structure.

**This work is dedicated to my parents and to my brother, without whose support this work
would not have been possible.**

ACKNOWLEDGEMENTS

I would like to express my deep sense of gratitude to my advisor Dr. Kris Berglund for his constant encouragement and support throughout the course of this work.

I would also like to thank my friends and colleagues Joel Dulebohn and Todd Werpy for their useful suggestions and help during this work.

Special thanks are due to Kathy Severin for her help in using X-Ray photoelectron spectroscopy.

TABLE OF CONTENTS

List of Tables	viii
List of Figures	ix
1. Introduction	1
1.1 Scope	1
1.2 Maleic anhydride and its importance	1
1.3 Specifications	4
1.4 Uses	4
1.5 Production	5
1.6 Objectives	8
2. Literature Survey	
2.1 Commercial technologies	9
2.1.1 Benzene route	9
2.1.2 Butane route	13
2.1.3 Butylene route	13
2.2 Alternate technology proposed	14
2.3 Characterization of catalysts	19
2.3.1 Bulk properties	20
2.3.2 Particle properties	21
2.3.3 Surface properties	23
2.3.4 Activity	24

3. Materials and Methods	25
3.1 Preparation of the catalysts	25
3.1.1 Experimental setup	25
3.1.2 Catalyst preparation	25
3.1.3 Commercial catalysts	28
3.2 Testing of the catalysts	29
3.2.1 Reactor setup	29
3.2.2 Product analysis	29
3.2.3 Experiments	34
3.3 Characterization of catalysts	35
3.3.1 Surface area analysis	35
3.3.2 X-ray diffraction analysis	36
3.3.3 Bulk composition analysis	37
3.3.4 Surface composition analysis	38
4. Results and Discussions	40
4.1 Testing of commercial catalysts	40
4.2 Testing of synthetic molybdenum oxide based catalysts	42
4.3 Testing of synthetic iron phosphate based catalysts	43
4.3.1 Effect of temperature on conversion	43
4.3.2 Effect of contact time on conversion	46
4.3.3 Effect of feed concentration on conversion	46
4.3.4 Effect of oxygen concentration on conversion	48
4.3.5 Effect of time on-stream on conversion	50
4.4 Results of characterization experiments	53
4.4.1 Surface area measurements	53
4.4.2 Bulk compositions	55

4.4.3 Surface compositions	57
4.4.4 Bulk crystal structure determination	57
5. Conclusions	62
6. Recommendations for future work	64
7. Appendices	
A. Laboratory synthesis procedure for the catalysts	68
B. X-ray diffraction spectra of the catalysts	71
8. List of References	78

LIST OF TABLES

Table 1.1	Physical properties of maleic anhydride	2
Table 1.2	Breakdown of the end uses of maleic anhydride	5
Table 2.1	List of major maleic anhydride producing companies	10
Table 3.1	Summary of catalysts synthesized	27
Table 3.2	Commercial catalysts tested	28
Table 4.1	Performance of commercial catalysts	41
Table 4.2	Performance of synthetic molybdenum based catalysts	43
Table 4.3	Surface areas of catalysts	55
Table 4.4	Bulk molar compositions of the catalysts	56
Table 4.5	Surface molar compositions of the catalysts relative to iron content	58

LIST OF FIGURES

Figure 1.1	Chemical structure of maleic anhydride	3
Figure 1.2	Conversion of succinic acid to maleic anhydride	6
Figure 1.3	Conversion of isobutyric acid to methacrylic acid	7
Figure 2.1	Halcon Design for the manufacture of maleic anhydride from Benzene or Butane	11
Figure 2.2	Idealized mechanism of oxidative dehydrogenation	15
Figure 3.1	Reactor setup	30
Figure 3.2a	NMR spectrum showing 5% succinic acid and 5% maleic acid standards	32
Figure 3.2b	NMR spectrum of the reaction products of the oxydehydrogenation reaction of succinic acid to maleic acid over a supported iron phosphate catalyst	33
Figure 4.1	Effect of temperature on the conversion of succinic acid to maleic acid using iron phosphate catalysts under the following conditions: a) contact time = 4 s, b) WHSV = 0.8-0.9 gm feed/gm catalyst/hr, c) feed concentration = 40 g/l, d) oxygen to feed mol ratio = 10:1, and e) time on-stream = 30 minutes	45
Figure 4.2	Effect of contact time on the conversion of succinic acid to maleic acid using iron phosphate catalysts under the following conditions: a) temperature = 475 °C, b) WHSV = 0.8-0.9 gm feed/gm catalyst/hr, c) feed concentration = 40 g/l, d) oxygen to feed mol ratio = 25:1, and e) time on-stream = 15 minutes	47

Figure 4.3	Effect of feed concentration on the conversion of succinic acid to maleic acid using iron phosphate catalysts under the following conditions: a) contact time = 4 s, b) WHSV = 0.8-0.9 gm feed/gm catalyst/hr, c) temperature = 475 °C, d) oxygen to feed mol ratio = 25:1, and e) time on-stream = 15 minutes	49
Figure 4.4	Effect of oxygen concentration on the conversion of succinic acid to maleic acid using iron phosphate catalysts under the following conditions: a) contact time = 4 s, b) WHSV = 0.8-0.9 gm feed/gm catalyst/hr, c) feed concentration = 40 g/l, and d) time on-stream = 15 minutes	51
Figure 4.5	Effect of time on-stream on the conversion of succinic acid to maleic acid using iron phosphate catalysts under the following conditions: a) contact time = 4 s, b) WHSV = 0.8-0.9 gm feed/gm catalyst/hr, c) temperature = 475 °C, d) feed concentration = 40 g/l, and e) oxygen to feed mol ratio = 25:1	52
Figure 4.6	Typical BET plot for a supported and promoted iron phosphate catalyst	54
Figure 4.7a	X-Ray diffraction spectrum of an iron phosphate catalyst, calcined at 110 °C	60
Figure 4.7b	X-Ray diffraction spectrum of an iron phosphate catalyst, calcined at 500 °C	61
Figure B-1	X-Ray diffraction spectrum of an iron phosphate catalyst, supported by LUDOX ® HS 40%; calcined at 110 °C	72
Figure B-2	X-Ray diffraction spectrum of an iron phosphate catalyst, supported by LUDOX ® HS 40%; calcined at 500 °C	73
Figure B-3	X-Ray diffraction spectrum of an iron phosphate catalyst promoted with cerium; calcined at 110 °C	74
Figure B-4	X-Ray diffraction spectrum of an iron phosphate catalyst promoted	75

with cerium; calcined at 500 °C

- Figure B-5** X-Ray diffraction spectrum of an iron phosphate catalyst supported by LUDOX ® HS 40% and promoted with cerium; calcined at 110 °C 76
- Figure B-6** X-Ray diffraction spectrum of an iron phosphate catalyst supported by LUDOX ® HS 40% and promoted with cerium; calcined at 500 °C 77

1. INTRODUCTION

1.1 Scope

With the ever increasing cost of fossil fuels, especially that of petroleum, there is a need to develop newer and more efficient technologies which are better able to use alternate feedstocks. Most of the chemical technologies present today are based on non-renewable energy and feedstock sources like fossil fuels. As the consumption of these products increase, a strain is placed on the fossil fuel sources due to increased production. Furthermore, it is well known that the worldwide stock of fossil fuels has a finite lifetime; therefore, it is imperative that we reduce our dependence on non-renewable feedstocks. One option is to replace conventional non-renewable feedstocks with renewable ones. The production of maleic anhydride, an important chemical, from a completely domestic, renewable fermentation derived source affords one such opportunity. The development of this technology will hopefully pave the way for other technologies to be developed starting from a fermentation feedstock. Therefore, the aim of this project is to develop a suitable heterogeneous catalyst for the production of maleic anhydride from a fermentation feedstock and to characterize it.

1.2 Maleic anhydride and its importance

Maleic anhydride is an unsaturated dibasic acid anhydride used extensively in the chemical industry (Figure 1.1). Table 1.1 gives some of the important physical properties of maleic anhydride (Cooley et al., 1983, Robinson et al., 1983).

Table 1.1 Physical properties of maleic anhydride

Empirical formula	$C_4H_2O_3$
Formula weight	98.06
Melting point, °C	52.85
Boiling point, °C	202
Specific gravity (at 20/20 °C, solid)	1.48
Specific gravity (at 20/20 °C, molten)	1.3
Viscosity, cP, at 60 °C	1.6
at 150 °C	0.6
Heat of formation, kJ/mol	-470.41
Heat of combustion, MJ/mol	-1.390
Heat of vaporization, kJ/mol	54.8
Heat of fusion, kJ/mol	13.65
Heat of hydrolysis, kJ/mol	-34.9
Vapor pressure, mm Hg, at 44.0 °C	1
at 135.8 °C	100
at 202.0 °C	760
Flash point, °C: open cup	110
closed cup	102
Flammable limits, vol%, lower	1.4 - 3.4
upper	7.1
Color	White crystals or colorless liquid
Crystal structure	orthorhombic

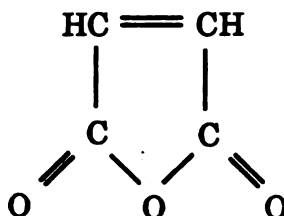


Figure 1.1 Chemical structure of maleic anhydride

The anhydride and the corresponding acid are industrially important raw materials in the manufacture of alkyd and polyester resins, surface coatings, lubricant additives, plasticizers, copolymers, and agricultural chemicals. The primary end use of maleic anhydride is as unsaturated polyester resins whose annual volume rose to 1.4 billion pounds in the U.S. in 1988 (Irving-Manshaw et al., 1989). The Chemical Products Synopsis (May 1988) predicts the average annual consumption of maleic anhydride in both the world and U.S. markets to rise steadily into the first half of the 1990's; one estimate predicts growth at 5.9% per year during the decade 1986-1995 (Irving-Manshaw et al., 1989). The U.S. annual demand for maleic anhydride was 370 million pounds in both 1987 and 1988.

The growing market for maleic anhydride has prompted a number of companies to increase their production of maleic anhydride. The major expansions planned in the U.S. itself amounts to almost 300 million pounds per year (Wood, 1990). All existing maleic anhydride production technologies are based on non-renewable feedstocks. The need to shift to renewable feedstocks coupled with the expansion in the market suggests the opportunity for a fermentation derived feedstock to compete with the existing technologies.

1.3 Specifications (Robinson and Mount, 1983)

Maleic anhydride is specified as a white fused mass or briquettes with a minimum crystallizing point temperature of 52.5 °C, complete and clear solubility in water (4 gms per 10 ml water), and a minimum assay of 99.5% (ASTM D 3504-76). The color of the melt is 20 APHA maximum, with a maximum APHA color of 40 after 2 hours of heating at 140 °C. ASTM method D 3366-74 describes the standard test for determining the color of maleic anhydride in the molten state.

1.4 Uses

The largest and most important use of maleic anhydride is in the manufacture of unsaturated polyester resins. On being reinforced with glass fiber, these can be used in the construction of boats, automobiles, trucks, buildings, piping, and electrical goods. The advantages of using reinforced resins as the material of construction are their corrosion resistance, light weight, and mechanical strength.

Maleic anhydride is the principal raw material for the production of fumaric acid, used primarily in the manufacture of sizing resins for newspapers. Fumaric acid is also used in the manufacture of unsaturated polyester resins, alkyd resins, quick-setting inks, and as a food acidulant. Maleic anhydride is also used in the manufacture of malic acid which is used as a beverage and food acidulant.

Maleic anhydride is used to manufacture lube-oil additives like ashless dispersants. Copolymer products of maleic anhydride are made by reaction with styrene, ethylene, and methyl vinyl ether.

The use of maleic anhydride in agricultural products includes its use in the manufacture of herbicides, fungicides, insecticides, and various plant growth regulators. Table 1.2 gives the breakdown of its various end uses (Robinson and Mount, 1983).

Table 1.2 Breakdown of the end uses of maleic anhydride

USES	%
Unsaturated polyester resins	55
Fumaric and Malic acids	9
Agricultural chemicals	9
Lube oil additives	9
Maleic co-polymers	5
Other uses	13

1.5 Production

Traditionally, maleic anhydride is produced from petroleum feedstocks. Benzene and butane are the most common feedstocks. However, as outlined before, the aim of this project is to develop a process which uses a fermentation feedstock to produce maleic anhydride. One such possible feedstock is succinic acid which can be produced from a fermentation process.

The Michigan Biotechnology Institute possesses a proprietary process for the manufacture of succinic acid using carbohydrates as a feedstock. The carbohydrates may be derived from corn or other agricultural materials which represent an abundant, renewable, low cost feedstock. The conversion to succinic acid utilizes an anaerobic fermentation process with an approximate product yield of 90% based on carbohydrate feedstock. Also, the separation and purification processes involved are relatively low cost .

It has been estimated at the Michigan Biotechnology Institute that the manufacturing cost of succinic acid is 29 cents per pound for a plant producing 150 million

pounds of succinic acid a year. This is based on 8 cents per pound carbohydrate, chemical costs as listed in the Chemical Marketing reporter, \$3 per million BTU steam cost and 3.2 cents per kwhr electricity cost. Fixed costs including maintenance and administration are 2.7 cents per pound of succinic acid. The capital cost estimated for a production plant of this capacity is 40 million dollars. On the other hand, the Chemical Product Synopsis of May, 1988 quoted the list price for maleic anhydride as 55 cents per pound, while the average sale price was estimated to be 47 cents per pound. The spot market price in August, 1990 was 57 cents per pound. With these estimates, it is realistic to develop a process which utilizes succinic acid as a starting material for the production of maleic anhydride.

The overall reaction from succinic acid to maleic anhydride that is proposed in this work is depicted in Figure 1.2.

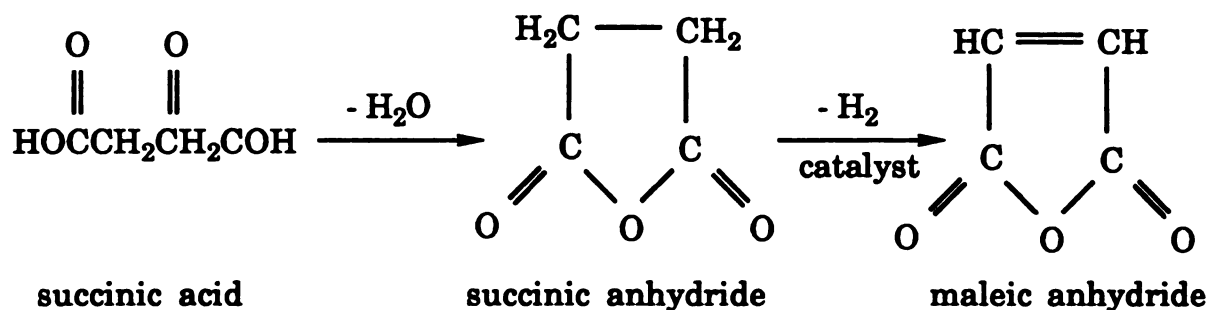


Figure 1.2 Conversion of succinic acid to maleic anhydride

Succinic acid can be readily dehydrated to succinic anhydride by the application of heat. Figure 1.2 shows the dehydration of succinic acid to succinic anhydride, which is believed to be an intermediate, followed by the dehydrogenation of succinic anhydride to maleic anhydride. This reaction is believed to occur in the presence of a catalyst and it is the object of this work to develop a catalyst suited for this reaction. The melting and boiling

points of each of the compounds named are sufficiently high that a vapor phase reaction is feasible for the proposed conversion.

An extensive literature search provided no information on the conversion of succinic anhydride to maleic anhydride as proposed. In light of this, it was decided that an analogous system be studied in which the conversion was similar to the reaction of interest. The analogous reaction scheme chosen was the conversion of isobutyric acid to methacrylic acid via oxydehydrogenation, depicted in Figure 1.3. This particular reaction was chosen due to several reasons. The similar dehydrogenation of a carbon-carbon bond adjacent to a

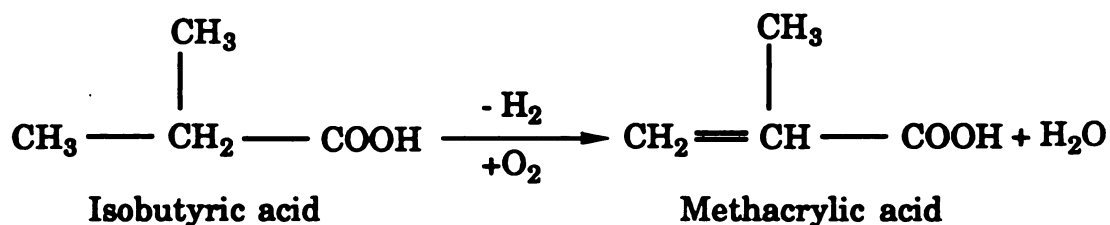


Figure 1.3 Conversion of isobutyric acid to methacrylic acid

carboxylic group and sufficient success in the development of appropriate heterogeneous catalysts as discussed in detail in the next chapter are some of the important attractive features. Also, as is evident in the literature, the temperature range involved is moderate, vapor phase reaction is possible, catalysts used (usually iron phosphate based) are relatively inexpensive, and the conversions and selectivities achieved are reasonably good. It was thus decided to base the proposed reaction on this analogous system.

1.6 Objectives

The main objective is to determine whether the production of maleic anhydride from succinic anhydride is technically feasible, and if so, to determine the best catalyst for the purpose and to characterize it.

2. LITERATURE SURVEY

2.1 Commercial technologies

Maleic anhydride is not found in nature. It was first prepared by Pelouze in 1834 by heating malic acid (Cooley et al., 1983). In more modern times, benzene had been the predominant feedstock from the start of commercial production until 1974 with a switch to n-butane as the feedstock of choice. This change was brought about by more favorable economics for butane and also by the recognition of health risks associated with benzene. Although all plants in the U.S. have switched over to butane, many plants across the world still run on benzene. Minor amounts of maleic anhydride are made from butene feedstocks or are recovered as a by-product of phthalic anhydride manufacture. Of present installed world capacity, 51% is based on benzene, 41% on butane, 5% on butenes, and 3% is by-product. Table 2.1 shows the major world manufacturers (Cooley et al., 1983).

2.1.1 *Benzene route (Robinson and Mount, 1983):*

Halcon (Scientific Design Co.) technology currently accounts for over 60% of the world capacity which uses the classical benzene route. Figure 2.1 shows the flow diagram of the process. A plant typically consists of a tubular reactor, an absorber, a partial condenser, a dehydrating unit, a refining column, and may or may not have a benzene recovery unit. The tubular reactor typically is a multitubular, fixed bed reactor which uses a molten salt mixture for cooling. Usually, the reactor is made of mild steel and can contain, depending on the capacity, over 15,000 tubes, each being about 25 mm in diameter and up to 4 m in length.

Table 2.1 List of major maleic anhydride producing companies

Company	Location	Capacity (thousand MTA)	Feedstock
Monsanto Co.	Pensacola, U.S.A	77	Butane
Huls AG	Bottrop, Germany	40	Benzene
Nippon Shohubai K.K.	Himeji, Japan	36	Benzene
Amoco Chemicals Co.	Joliet, U.S.A.	34	Butane
Alusuisse Italia	Bergamo, Italy	33	Benzene
Ashland Chemical Co.	Neal, U.S.A.	23	Butane
Mobay Synthetics Corp.	Houston, U.S.A.	23	Butane
Aristech.	Neville Island, U.S.A.	20	Butane
Mitsubishi Chemicals	Mizushima, Japan	18	Mixed C ₄ 's
CdF Chimie	Villers-Saint Paul, France	15	Benzene
Nichiyu Chemical Co. Ltd.	Oita, Japan	15	Butane
Takeda Chemical Industries Ltd.	Kashima, Japan	15	Benzene

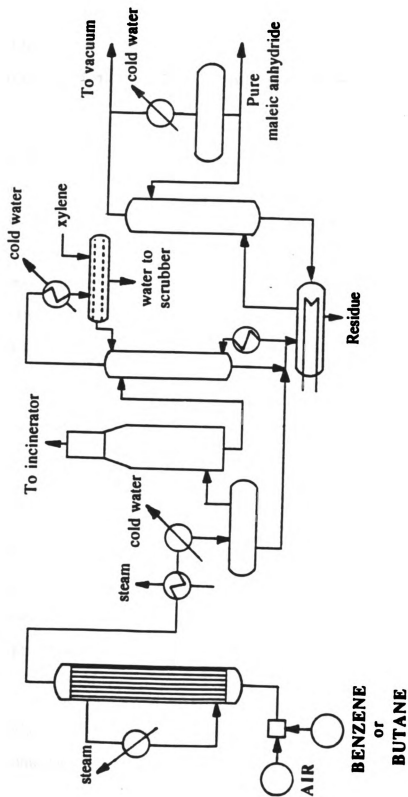


Figure 2.1 Halcon Design for the manufacture of maleic anhydride from Benzene or Butane

A 1-1.4 mol% concentration of benzene in air is passed through the catalyst at 60-130 grams benzene per liter of catalyst per hr. The molten salt cooler produces steam which maintains the temperature of the salt from 350 °C to 400 °C. Pressure is maintained at 1 to 2 atm. Steam is produced in heat exchangers that cool the effluent gas from the reactors. Yields as high as 75 mol% have been reported.

The majority of commercial benzene oxidation catalysts are supported. The support may be metal shapes or low surface area supports, for example, ceramically bonded alumina, silica, or carborundum. The active component of the catalyst, which contains a number of vanadium oxides, usually is mudded onto the carrier by concentration from a solution. This gives a catalyst with about 1-2 m²/gm of surface area. The promoting element is usually molybdenum. Other elements that have been tested include phosphorus, tin, boron, silver, titanium, tungsten, nickel, cobalt, and various alkali and alkaline earth metals.

An important part of the process is the recovery and purification of the final product from the reactor gas, which typically contains about 1% maleic anhydride. The gas is cooled to below 200 °C in heat exchangers; then it is further cooled to near the dew point of water which is 55-60 °C under these conditions. About 40 to 60% of the maleic anhydride is condensed which is then separated from the gas stream. A major problem is that the maleic anhydride absorbs water, forming maleic acid which tends to isomerize to the more stable isomer, fumaric acid. This clogs the system and limits the amount that can be condensed initially. The remaining maleic anhydride is then recovered as the acid by absorption in water.

The maleic acid solution is concentrated and dehydrated to crude maleic anhydride directly or by the use of entraining agents like o-xylene. Here, yield losses and downtime can occur as a result of blockages with fumaric acid and tar. Effluent gases

contain unreacted benzene, carbon monoxide, and trace impurities. These contaminants may be oxidized thermally or catalytically and carbon absorption may be used to recover the benzene for recycling. The condensed or dehydrated crude maleic anhydride is fractionated under reduced pressure to the finished product by either batch or continuous distillation.

2.1.2 Butane route (Robinson and Mount, 1983):

Monsanto was the first commercial producer of maleic anhydride from a butane feedstock in 1974. The processing methods, the conditions, and restraints are generally governed by the similar factors as has been described for the benzene route. The greater ratio of water-to-anhydride formed in the butane route causes lesser amounts of maleic anhydride to be recovered by condensation as a liquid than in the benzene route.

The major point of interest here is the catalyst used. Phosphorus-vanadium-oxygen (PVO) is the the most widely claimed type. Numerous patents using different promoters have been issued. The elements experimented with as a promoter include iron, chromium, titanium, cobalt and/or nickel, zirconium, zinc, molybdenum, copper, and many others.

2.1.3 Butylene route:

A butylene containing stream from naphtha cracking is used as the feedstock which involves using a modified PVO catalyst system. A fluidized bed reactor can be used for the production of maleic anhydride which offers certain advantages. These include efficient removal of reaction heat, easy maintenance of optimum reaction temperatures, long catalyst life, and more economical and easy to construct reactors on a larger scale. In this process, the slow rate of dehydrogenation of n-butane to butylenes is the rate determining step.

The catalyst involved here is, as for the other processes, a modified PVO system. Modifying elements tested include titanium and/or tungsten, molybdenum, copper

and/or niobium, uranium, lithium and other alkali metals, silver, silicon, and zirconium. Other systems studied include vanadium-arsenic, vanadium-titanium, vanadium-molybdenum and/or cobalt, phosphorus-tungsten, phosphorus-molybdenum, molybdenum, and molybdenum-tungsten-antimony (Robinson and Mount, 1983).

2.2 Alternate technology proposed

As mentioned in the previous chapter, an alternate pathway to the production of maleic anhydride from fermentation derived succinic acid is proposed in this work. An idealized reaction for this pathway is depicted in Figure 1.2.

An extensive literature search provided no citation for the proposed reaction. In light of this, it was decided that an analogous system be studied in which the conversion was similar to the reaction of interest. The analogous reaction scheme chosen was the conversion of isobutyric acid to methacrylic acid via oxydehydrogenation. This reaction is depicted in Figure 1.3. The specific reaction scheme of converting isobutyric acid to methacrylic acid was developed by Ashland Chemical and is believed to have been brought on line in 1989 (Szmant, 1989). This reaction was chosen as the model on which to base the desired reaction due to several reasons. The similar dehydrogenation of a carbon-carbon bond adjacent to a carboxylic group, sufficient success in the development of appropriate heterogeneous catalysts, and its commercial feasibility are some of the important attractive features. The reason that oxidative dehydrogenation is chosen over conventional dehydrogenation is that a study of the thermodynamics reveals a much more favorable pathway for the reaction in the presence of oxygen as the equilibrium is shifted. Also, the free energy change tends to be negative in the presence of oxygen and positive in its absence, which is favorable. In some cases, the presence of oxygen also greatly increases the equilibrium constant. Although the exact mechanism of oxidative dehydrogenation is not completely understood, an idealized mechanism for the reaction is presented in Figure 2.2 (Hightower, 1990). The example chosen is that of the oxydehydrogenation of

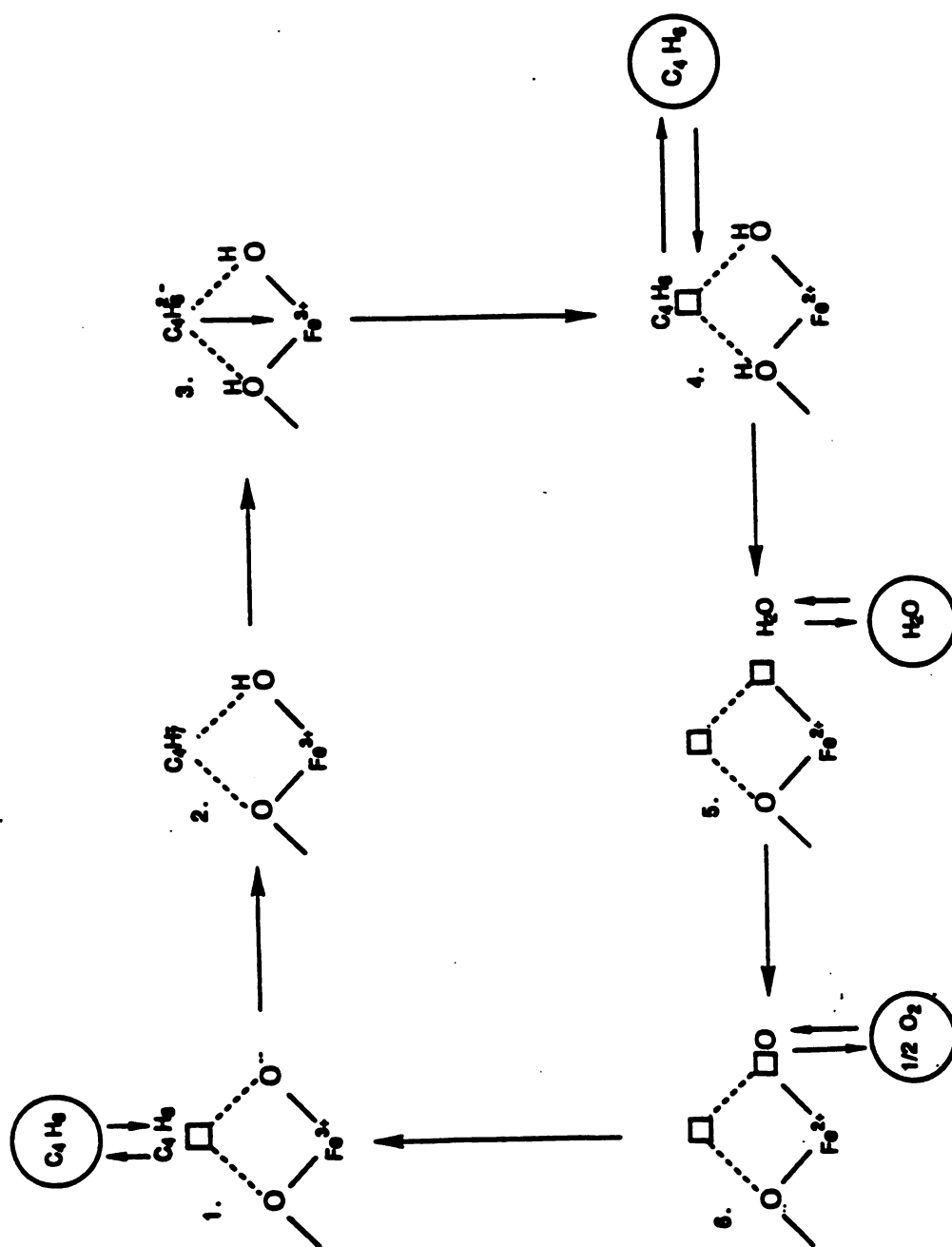


Figure 2.2 Idealized mechanism of oxidative dehydrogenation

butane to butene over an iron based catalyst. The first step shows the adsorption of the reactant molecule onto an active site on the catalyst. The next two steps show the releasing of the hydrogens and their subsequent reaction with surface oxygen resulting in dehydrogenation. The last two steps show the removal of water and the regeneration of the oxygen sites on the catalyst surface. This idealized sequence indicates possible avenues for the optimization of the process.

Obviously, the most important step in the whole reaction scheme is the catalytic oxidative dehydrogenation of isobutyric acid. Numerous patents have been issued for different catalysts developed for this reaction.

Watkins (1974) developed a catalytic process for the manufacture of unsaturated acids and esters wherein lower aliphatic acids like isobutyric acid and esters like methyl isobutyrate are dehydrogenated in the presence of oxygen and a solid dehydrogenation catalyst at a range of temperatures from 250 °C to about 600 °C. The catalyst used was a calcined residue of the mixed phosphates of iron and lead. Watkins (1975) also developed a catalyst which was a calcined residue of a mixture of bismuth oxynitrate, iron phosphate, and lead phosphate.

Statz and co-workers (1980) patented a catalyst containing alkali metal, chromium, iron, lead, phosphorus, and oxygen which was used for the oxidative dehydrogenation of isobutyric acid. It was based on the discovery of a phosphate catalyst containing the aforementioned elements to be particularly well suited for dehydrogenation reactions used to produce unsaturated acids and esters like methacrylic acid. Both fixed bed and fluidized bed were tried with success. For the reaction of isobutyric acid to methacrylic acid, the catalysts were tested at 400 °C at different contact times and conversions between 20% and 60% were achieved. The selectivity to methacrylic acid was between 40% to 85%.

Daniel and Brusky (1981a) of Ashland Oil, Inc., developed a vapor phase reaction wherein isobutyric acid or a functional equivalent, for instance, a lower alkyl ester was oxidatively dehydrogenated to the corresponding α,β - ethylenically unsaturated derivative by contact with a heterogeneous catalyst in the presence of molecular oxygen. The catalyst used was composed of calcined phosphates of iron containing silver as a modifier or dopant component. An optimum temperature range of 375 °C to 475 °C with contact times of less than a second provided extremely high conversions of isobutyric acid from 74% to 96% with a selectivity to methacrylic acid of over 60%. Daniel and Brusky (1981b) developed another catalyst composed of calcined phosphates of iron containing tellurium as a modifier. These catalysts were tested at about 400 °C and a contact time of about 0.3 seconds and gave a conversion of about 77% to 87% with a selectivity of about 70%. Daniel (1982) also developed a catalyst composed of calcined phosphates of iron, silver, and niobium. At about 400 °C and a contact time of about 0.5 second, conversions of 40% to 80% with a selectivity to methacrylic acid of over 70% were obtained.

Ruszala (1983a) developed a catalyst for the same reaction which was composed of the calcined oxides of iron and at least two members selected from the group consisting of antimony, niobium, tantalum, and tungsten. A support was used which constituted anywhere between 5% and 95% by weight of the finished catalyst. A host of supports were tried which included alumina, pumice, silicon carbide, zirconia, titania, silica, alumina-silica etc. At a reaction temperature of around 415 °C and a contact time of less than a second, conversions from 15% to 32% were obtained while the selectivity to methacrylic acid was around 50%.

Daniel and Brusky (1983a) used a catalyst composed of calcined phosphates of iron containing cobalt or lanthanum as a modifier. Using similar conditions of temperature and contact time as Ruszala, they achieved extremely high conversions of up to 99% with a

selectivity of around 60%. It was noticed that a high conversion also implied a lower selectivity towards the desired product.

Ruszala (1983b) used a catalyst composed of the calcined oxides of uranium and tungsten. The highest conversion achieved with this catalyst was 47% with a selectivity of 40% at a reaction temperature of 475 °C. Daniel (1983b) used a catalyst composed of the calcined phosphates of chromium, molybdenum, and tungsten. A silica support was also used. A reaction temperature of around 300 °C and a contact time of 0.5 seconds provided an optimum set of conditions for achieving conversions up to 90% and selectivities to methacrylic acid of up to about 70%. He also used a catalyst composed of the calcined phosphomolybdate of potassium and cerium (Daniel, 1983c). Supports tried included silica, alumina, quartz, titanium dioxide, carbon, silicon carbide, etc. A reaction temperature of 300 °C and a contact time of less than a second gave a conversion of isobutyric acid of about 79% and a selectivity to methacrylic acid of about 66%. Another catalyst tried was composed of the calcined phosphates of iron, silver, and chromium and a support material consisting of any one of silica, alumina, quartz, titanium dioxide, carbon, and silicon carbide (Daniel, 1983d). A reaction temperature of about 400 °C and a contact time of less than a second was used. Conversions of isobutyric acid from 84% to 96% with a selectivity to methacrylic acid from 66% to about 75% were achieved. Calcined phosphates of iron and cerium were also tried (Daniel, 1983e). Similar supports as indicated before were tried with success. A reaction temperature of 400 °C and a contact time of less than a second provided a conversion of 84% isobutyric acid with a selectivity towards methacrylic acid of about 85%.

Ruszala (1984) developed a catalyst composed of the calcined mixtures of salts of titanium and iron. Various supports were tried including colloidal silica or any other form of silica, alumina, pumice, zirconia, quartz, carbon, silicon carbide, etc. Reaction temperatures from about 400 °C to 450 °C were used with a contact time of less than a

second to achieve conversions of around 35% and selectivities around 45%. Daniel (1984) developed a catalyst composed of iron, phosphorus, silicon, vanadium, and molybdenum for the conversion of isobutyric acid to methacrylic acid. This catalyst also had a support as one of silica, alumina, quartz, titanium dioxide, carbon, silicon carbide, etc. A reaction temperature of 280 °C to 320 °C was considered optimum. With a contact time of about a second, a conversion of about 81% was achieved with a selectivity towards methacrylic acid of about 74%.

Pedersen and co-workers (1984) provide a process for the preparation of iron phosphorus mixed oxide catalysts with a promoter and a support. The iron and phosphorus containing compounds and promoter elements containing compounds, if any, are introduced into a substantially organic liquid medium, heated, separated and then dried and calcined. These catalysts are useful for the oxidative dehydrogenation of organic compounds such as aldehydes or carboxylic acids.

McGarvey and Moffat (1991) have studied the reaction over a series of ion exchange modified 12-heteropoly oxometalate catalysts. Watzenberger and co-workers (1990) have studied the deactivation of such heteropolyacid catalysts and suggest a way of eliminating deactivation of the catalyst.

2.3 Characterization of catalysts

Characterization of catalysts is of paramount importance in the development of any catalytic process. At each stage of the development, characterizing the catalyst not only checks the effectiveness of the catalyst, but also provides a standard for future products. According to Hanseal and Hanseal (1989), the goal of catalyst characterization should not only be an attempt to understand the catalytic act on a molecular level, but also to study the nature of the individual catalyst sites and their interdependence and interaction with one another as well as with the reactants.

The characterization process is usually divided into four parts. Bulk property measurements, particle property measurements, surface property measurements and activity measurements. Each will be discussed separately.

2.3.1 Bulk properties:

Complete qualitative and quantitative **component identification** within the catalyst is the first attribute that should be determined (Richardson, 1989). Besides the principal components added, contaminants should also be quantified. A host of techniques are available for the determination of bulk compositions. The most popular are spectroscopic methods which include x-ray fluorescence (Cullity, 1956), atomic absorption spectroscopy, inductively coupled plasma spectroscopy, and analytical electron microscopy (Richardson, 1989).

Phase structure identification is another important aspect which is relatively much more difficult to measure. X-ray diffraction is quite well developed for this application. Since each crystal phase gives a characteristic pattern, it is possible to identify all the phases in the sample. There are, however, some problems associated with this technique. A minimum amount of sample, depending on the atomic weight, is required and lines from different phases often occur at the same position, interfering with and overlapping each other (Richardson, 1989). Millet and co-workers (1990) have specifically studied the phase structure of iron phosphate catalysts used in the conversion of isobutyric acid to methacrylic acid. They studied the phase structure before and after the reaction to determine the phases present and confirmed that certain new and as yet unidentified phases had been formed. X-ray diffraction along with Mössbauer spectroscopy can also help in understanding the role of promoters in a catalyst. Millet and Verdine (1991) have used those techniques to explain the role of cesium in iron phosphate catalysts. Mössbauer spectroscopy can also be used to determine the oxidation state of iron before and after the

catalytic reaction as has been performed with iron phosphate catalysts to determine the most selective phase for the reaction (Millet et al., 1989).

Delannay (1984) has indicated that electron diffraction to identify phases is also possible during electron microscopy. The advantage of this technique is that the resolution is very high and so individual crystallites can be identified.

Thermal analysis for characterizing solid materials is based on the fact that, at a proper temperature interval, any solid will undergo characteristic phase transformations (Lemaitre, 1984). Differential thermal analysis (DTA) and thermal gravimetric analysis (TGA) are two of the most widely used thermal analytical techniques. The former measures energy changes as the sample is scanned through phase changes, while the latter records weight loss or gain (Richardson, 1989). The characteristic temperature at which a thermal change occurs in a given sample depends on the phase composition of the sample and the composition of the surrounding atmosphere as well as on any factor which affects the kinetics of the transformation.

2.3.2 *Particle properties:*

Density is an important particle property that needs to be evaluated. Density grading is a technique used to segregate catalyst particles based on their individual densities (Seamans et al., 1989). Richardson (1989) mentions four different ways in which densities may be defined. The *theoretical density* is the ratio of the mass of a collection of discrete pieces of solid catalyst to the sum of the volumes of each piece, if the solid catalyst has an ideal regular arrangement at the atomic level. X-ray diffraction can be used to measure the theoretical density. In defining *skeletal density*, the volume is taken as the sum of the volume of the solid material and any closed pores within the solid. A displacement pycnometer is used to measure the *particle density* in which the volume is taken as the sum

of volume of the solid, closed pores and accessible pores within the particle. The *packing density*, or the bulk density also considers the void space between the particles.

Particle size distribution can be determined, depending on the shape of the particles, by sieving, optical and electrical imaging, light scattering etc.

Mechanical properties can sometimes supersede outstanding catalytic activity and often are the limiting factors for using and regenerating industrial catalysts (Bertolacini, 1989). To evaluate the mechanical properties of catalysts, several test methods have been standardized by the ASTM D-32 Committee on Catalysts. These include tests on attrition and abrasion, single pellet crush strength, vibrated packing density, and particle size analysis (Bradley et al., 1989).

Surface area is perhaps the most important particle parameter specified irrespective of the type of surface (Richardson, 1989). The principles of physical adsorption are employed to calculate the specific surface area which is usually given in square meters per gram of catalyst. The linearized form of the famous Brunauer, Emmett, and Teller equation is used to calculate the surface area. Nitrogen adsorption experiments are the principal methods used. Surface areas of catalysts can range from 0.01 m²/gm to 1000 m²/gm or more. For example, some zeolite catalysts have extremely high surface areas of about a 1000 m²/gm while an iron alumina catalyst used for ammonia synthesis has a surface area of only 10 m²/gm (Richardson, 1989). Sing (1980) has recommended a general procedure for the analysis of physisorption measurements on catalysts.

Pore size distribution has become an essential feature of particle characterization (Lecloux et al., 1981). These are required to properly estimate pore mouth poisoning, pore diffusional resistances, and deactivation control. Usually, macropores are measured with mercury porosimeters, whereas mesopores and micropores are measured with nitrogen adsorption-desorption isotherms (Richardson, 1989).

Although measuring the diffusivity of catalysts with a high degree of accuracy is quite difficult, nevertheless it is important to know the diffusion coefficient for the calculations of effectiveness factors. The classical method of measuring diffusivity is the Wicke-Lallenbach technique, although chromatographic techniques have also been used (Richardson, 1989).

2.3.3 *Surface properties:*

Since the surface of the catalyst is the active part in any catalytic reaction, measurement of surface attributes is of paramount importance to understand the behavior of the catalyst. The important features to be characterized include morphology and composition, structure, dispersion, and acidity. These are further discussed.

Morphology involves the study of the shape and size of the catalysts. Numerous techniques are available, the primary ones being Scanning Electron Microscopy (SEM), Transmission Electron Microscopy (TEM), Scanning Transmission Electron Microscopy (STEM), X-ray diffraction, Extended X-ray Absorption Fine Structure (EXAFS), Auger Electron Spectroscopy (AES), X-ray Photoelectron Spectroscopy (XPS), and Ultraviolet Photon Spectroscopy (UPS) to name a few. Delgass and co-workers (1979) provide an excellent description of various spectroscopic techniques involved. Cohen (1990) has used x-ray diffraction to obtain statistical information on the nature of catalysts and on the structure of micron-sized single crystal particles.

Structure identification of the surface phases is best accomplished by electron microscopy using either an SEM or TEM or both. The advantage in using electron microscopy is that since electrons interact much more strongly with matter than do X-rays or neutrons, they can be scattered appreciably by extremely small atomic clusters (Howie, 1980). This technique is often used complimentary to Auger Electron Spectroscopy or X-ray Photoelectron Spectroscopy.

Dispersion of the active fraction of the catalyst is defined as the ratio of the number of active atoms exposed at the surface to the total number of active atoms present in the catalyst. The experimental techniques used to measure dispersion include chemisorption techniques, X-ray diffraction and scattering, Transmission Electron Microscopy, and XPS peak intensity measurements (Lemaitre et al., 1984).

Acidity measurements include measuring the type of acidity, the acid strength, and the distribution of acid strengths (Richardson, 1989). Jacobs (1984) has provided a detailed account of the various techniques available to measure the acidities of catalysts.

2.3.4 *Activity:*

Kinetic activities are based on the rate equations for the reaction under study. For this reason, it is essential to conduct kinetic experiments to determine the exact rate equation first. Once the rate equation is available, the activity can be expressed either as a rate, a rate constant or an Arrhenius constant (Richardson, 1989).

To measure the kinetic rate data, different types of experimental reactors may be used. Tubular reactors can be operated in either a differential or an integral mode. Spinning basket or internal recycle reactor is very commonly used for measuring kinetic data (Kenney, 1980). Batch reactors are usually employed for liquid phase reactors using slurried catalysts. Pulse reactors are simple and fast reactors that offer economy of feed and provide protection against process deactivation (Richardson, 1989).

Müller-Erlwein and Hofmann (1988) have considered the problem of evaluating kinetic parameters from dynamic experiments for the heterogeneously catalyzed oxidative dehydrogenation of isobutyric aldehyde to methacrolein.

3. MATERIALS AND METHODS

The project was essentially divided into three stages: a) preparation of the catalysts, b) testing of the catalysts, and c) characterization.

3.1 Preparation of the catalysts

3.1.1 *Experimental Setup:*

The catalysts were prepared in accordance with the experimental techniques mentioned in the various patents describing the conversion of isobutyric acid to methacrylic acid, discussed in detail in the last chapter. A wide mouthed flask was used as the reaction vessel with a refluxing column and a condenser attached to it. The reaction mixture was constantly stirred and the vapors refluxed using cooling water in the reflux column. Refluxing was continued for about 24 hours after which the reaction was considered to be complete. The excess water in the system was distilled off. The resulting thick paste obtained was dried in an oven overnight at about 110 °C. The catalyst was removed from the reaction vessel and calcined in an oven. Calcination was carried out in air at 450 °C for six hours and further calcined in a mixture of nitrogen and oxygen at 500 °C for two hours.

3.1.2 *Catalyst preparation:*

Two general categories of catalysts were prepared. The first were catalysts which had a molybdenum oxide base whereas the second had an iron phosphate base. In the latter category, four different types of catalysts were prepared, each having a different composition: the first was the base iron phosphate catalyst, the second had a support (LUDOX® HS 40%) added to the base, the third had a promoter (lanthanum or cerium) added to the base, and the fourth had both the support and the promoter added to the base.

Table 3.1 gives a summary of the various catalysts prepared and their constituents. All chemicals used were bought from Aldrich Chemical Co., except for the silica support LUDOX[®] HS 40% (DuPont Chemicals), iron nitrate nonahydrate (Columbus Chemical Industries, Inc.), and heavy water (Cambridge Isotope Laboratories).

A typical iron phosphate catalyst preparation which has all the ingredients: the base catalyst, a support, and a promoter is described as an example. The preparation follows the techniques available in patent literature (Daniel, 1983e).

Forty eight and a half grams of iron nitrate nonahydrate was mixed with 15 ml phosphoric acid, 120 ml distilled water, 10 ml LUDOX[®] HS 40% as the support, and 2.6 grams of cerium nitrate hexahydrate as the promoter. The chemicals were put in a reaction vessel and refluxed while being continuously stirred. Refluxing was continued for almost 24 hours after which the reaction was deemed complete. It was assumed that all the iron nitrate would have reacted with the phosphoric acid to produce the phosphate while the silica support (LUDOX[®] HS 40%) and the cerium promoter would have embedded into the crystal structure of the catalyst. The slurry obtained was heated for about two hours in order to distill off the excess water. The thick paste formed was dried for about 24 hours at 110 °C. The catalyst obtained was calcined at 450 °C in air at a furnace available at the Composite Materials and Structures Center, Michigan State University. The catalyst was further calcined in the presence of a mixture of nitrogen and oxygen at 500 °C in the reactor at the Michigan Biotechnology Institute.

The other iron phosphate catalysts were prepared in exactly the same way, except that the silica support and the cerium or lanthanum promoter was added only when so desired. Detailed preparations for all catalysts are given in Appendix A.

Table 3.1 Summary of catalysts synthesized

Catalyst	Constituents
Iron phosphate based	
1) Base catalyst	Iron, phosphorus, and oxygen
2) Base catalyst with support	Iron, phosphorus, oxygen, and silicon
3) Base catalyst with promoter	Iron, phosphorus, oxygen, and lanthanum as promoter
4) Base catalyst with promoter	Iron, phosphorus, oxygen, and cerium as promoter
5) Base catalyst with support and promoter	Iron, phosphorus, oxygen, silicon, and cerium
6) Base catalyst with support and promoter	Iron, phosphorus, oxygen, silicon, and lanthanum
Molybdenum oxide based	
1) Molybdate catalyst	Molybdenum, oxygen, phosphorus, vanadium, and copper.
2) Molybdate catalyst	Molybdenum, oxygen, phosphorus, vanadium, tungsten, and hydrogen.
3) Molybdate catalyst	Molybdenum, oxygen, phosphorus cerium, and potassium

The molybdenum oxide based catalysts were prepared using a molybdate compound instead of the iron phosphate. A typical preparation of a molybdate catalyst is described next. This preparation follows that described in the patent literature discussed earlier (Daniel, 1983c). Other preparations are given in Appendix A.

Thirty milliliters of distilled water was used as a solvent into which 1.72 grams of potassium hydroxide was dissolved. A thick slurry was made by mixing 27 grams of $(\text{NH}_4)_2\text{Mo}_7\text{O}_{24} \cdot 4\text{H}_2\text{O}$, 8.1 grams of $(\text{NH}_4)_2\text{Ce}(\text{NO}_3)_6$, and 3.2 ml of phosphoric acid. 30 ml of concentrated hydrochloric acid was added slowly to the slurry, which caused it change to a red color and then back to yellow. The yellow slurry was placed on a magnetic stirrer and heated at 125 °C for five hours. A thick paste was obtained which was placed in an oven to dry at 110 °C for 18 hours.

3.1.3 *Commercial catalysts:*

Commercially available standard dehydrogenation catalysts were also procured from United Catalysts Inc., Louisville, Kentucky. Table 3.2 lists these catalysts along with their constituents and form. Exact compositions are proprietary information.

Table 3.2 Commercial catalysts tested

CATALYST	CONSTITUENTS and FORM
United Catalyst G-84C	Iron, Potassium, Chrome ; 1/8" extrusions
United Catalyst G-65	Nickel on Refractory ; 1/8" extrusions
United Catalyst G-13	Copper Chromite ; 3/16" x 3/16" tablets
United Catalyst G-22	Copper Chromite ; 3/16" x 3/16" tablets
United Catalyst G-41	Chromium on Alumina ; 1/8" extrusions

3.2 Testing of the Catalysts

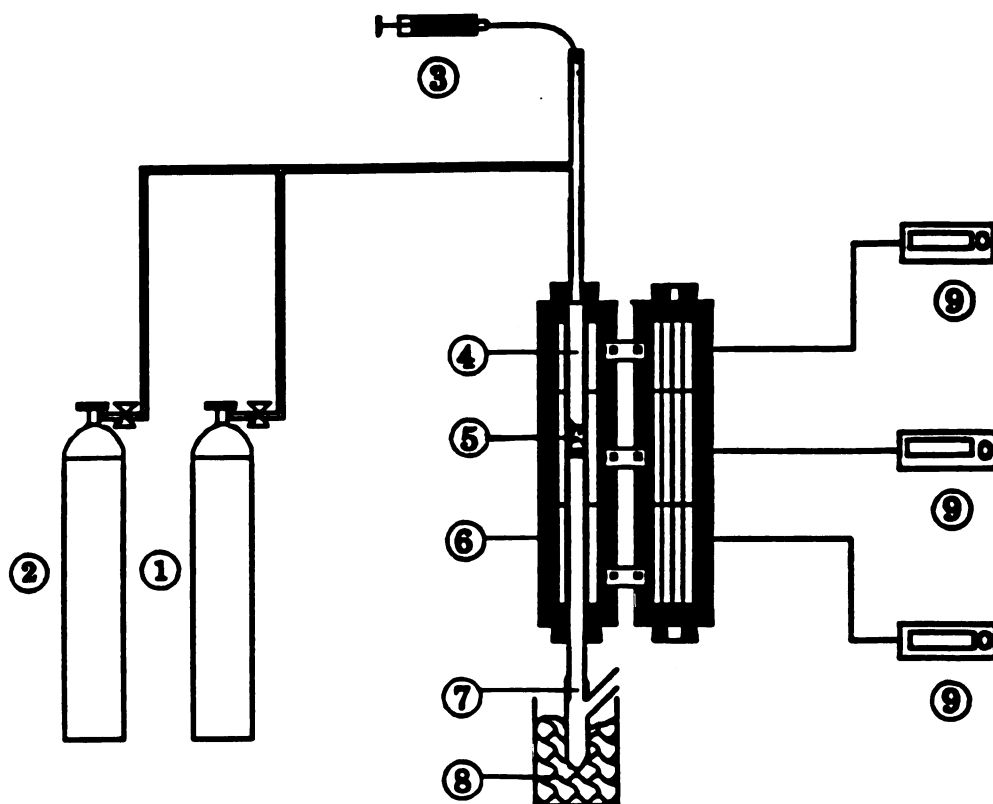
All the catalysts were tested in a reactor located at the Michigan Biotechnology Institute. The reactor setup is shown in Figure 3.1.

3.2.1 *Reactor setup:*

The reactor was a simple quartz tube with a glass frit attached at the center which served to act as a support for the catalyst. The reactor tube was enclosed inside a three zone furnace (series 3210, manufactured by Applied Test Systems, Inc.). The temperature of each zone of the furnace was independently controlled using Digi-Sense temperature controllers (model 2186-10, marketed by Cole-Parmer Instrument Company). A syringe infusion pump with adjustable flow rates, (model 11, manufactured by Harvard Apparatus), at the top of the reactor served to inject the succinic acid feed solution into the reactor. Glass wool was used to prevent any contamination on the frit. Glass beads were loosely packed on the glass wool up to the top of the reactor to provide a uniform flow of the feed on to the catalyst. Nitrogen was used as an inert carrier gas through the reactor. A provision was made to introduce oxygen into the reactor along with the nitrogen. The flow of the two gases was regulated by Brooks 5850E series mass flow controllers. The product gases from the reactor were condensed into a collection flask placed in an ice bath. The reaction products, collected on the sides of the collection vessel were dissolved in water and taken for analysis. Carbon dioxide production was monitored by routing the effluent gases to a flask containing a buffer solution of pH 5 into which an ORION (model 95-02) CO₂ electrode was immersed.

3.2.2 *Product analysis:*

Product analysis was done on a VXR 300 machine located at the Max T. Rogers facility at Michigan State University. ¹H nuclear magnetic resonance was the



- 1. Nitrogen gas cylinder
- 2. Oxygen gas cylinder
- 3. Syringe pump with feed
- 4. Reactor tube
- 5. Catalyst

- 6. Furnace
- 7. Collection vessel
- 8. Ice bath
- 9. Temperature controllers

Figure 3.1 Reactor setup

technique of choice because of the ease in identifying products and determining their composition. This technique permits the identification of all compounds regardless of their functionality. In this case however, maleic anhydride cannot be detected because of the large amounts of water in the system, which causes the hydration of the anhydride to the acid. So, the final detectable product was maleic acid. As the technique required a presence of a deuterated solvent to lock on, the succinic acid was dissolved in heavy water, D₂O, instead of regular water. Typical NMR spectra are shown in Figure 3.2. Figure 3.2a shows succinic and maleic acid standards at a concentration of 5% in D₂O; while Figure 3.2b shows the reaction products from a typical run over an iron phosphate catalyst. D₂O is highly hygroscopic, absorbing atmospheric water to form HDO. This shows up in the NMR spectra as the large solvent peak. Decoupling techniques were used to reduce the size of the large solvent peaks expected in all analyses. As is evident from comparing the two spectra, the formation of maleic acid is confirmed.

¹H NMR, as the name suggests, is actually a technique to measure the number of protons present in the sample (Delgass et al., 1979). As maleic acid has two protons less than succinic acid, the peak of maleic acid will be half that of succinic acid at the same concentrations. Therefore, to determine the relative amounts of the two, the area of the maleic acid peak had to be multiplied by two to equate it with the succinic acid peak. In Figure 3.2b, the numbers alongside the peaks indicate the area as obtained by the analysis. Since there was initially no maleic acid, all maleic acid present is as a result of conversion of succinic acid. As an example, the conversion to maleic acid is given as

$$\begin{aligned}\% \text{ Conversion} &= (0.19 \times 2) / \{(0.19 \times 2) + 1.09\} \times 100 \\ &= 25.8 \%\end{aligned}$$

The absence of any other detectable peak in the spectrum also indicates the high selectivity of the reaction. The only other reaction product possible which is not detectable

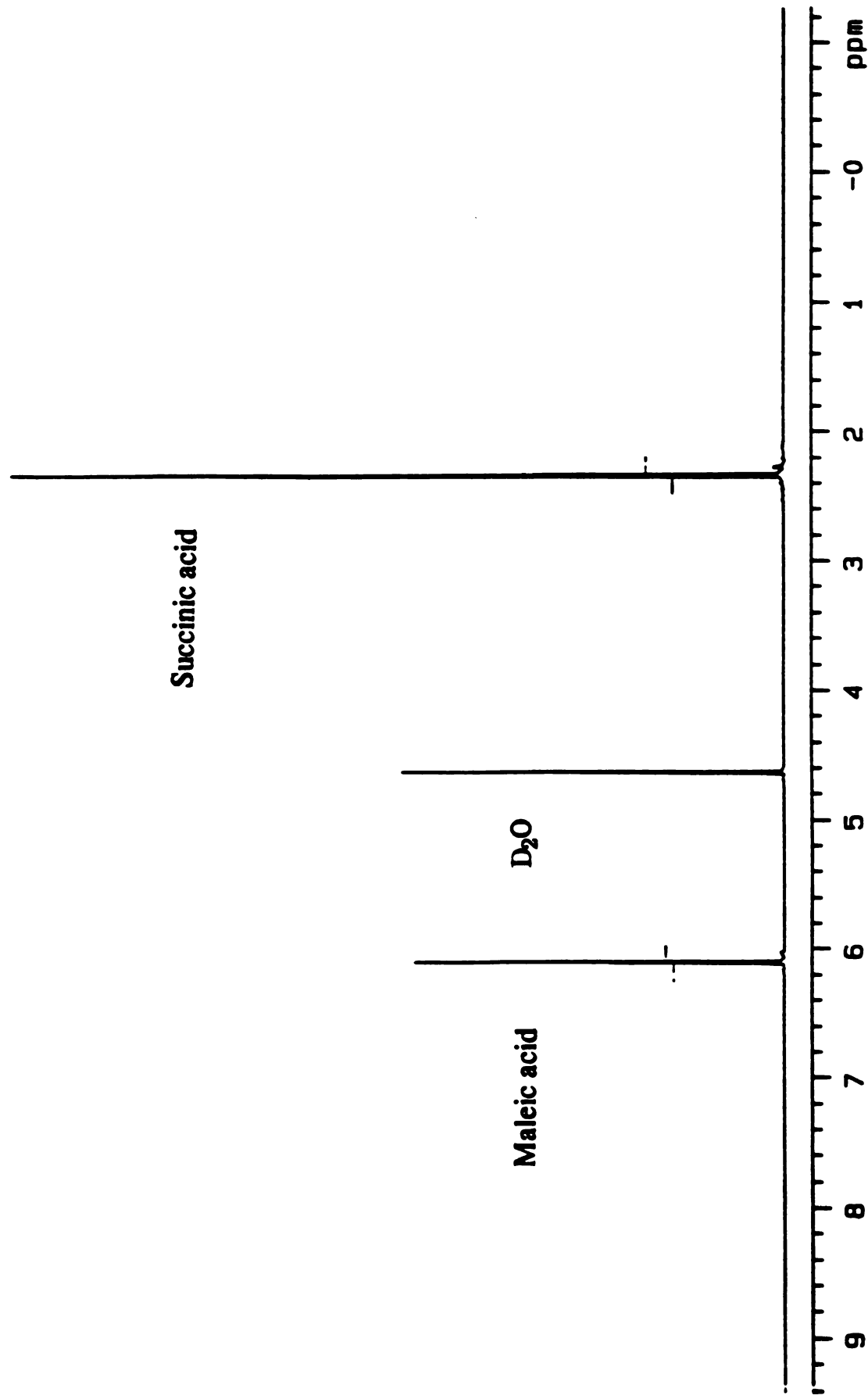


Figure 3.2a NMR spectrum showing 5% succinic acid and 5% maleic acid standards

Succinic acid

D₂O

Maleic acid

0.19

1.09

ppm

Figure 3.2b NMR spectrum of the reaction products of the oxydehydrogenation reaction of succinic acid to maleic acid over a supported iron phosphate catalyst

by ^1H NMR is carbon dioxide which could be produced if the succinic acid was being directly decarboxylated to CO_2 in the presence of oxygen. This possibility was monitored by the CO_2 electrode. The presence of CO_2 is indicated by a large change in the voltage reading by the electrode.

3.2.3 *Experiments:*

Experiments were conducted with commercially available dehydrogenation catalysts to determine if the conversion of succinic acid to maleic acid was possible with reasonable conversion and selectivities.

Subsequently, experiments were conducted with the catalysts prepared in the laboratory to determine their effectiveness in the proposed conversion. Thereafter, the effect of various parameters on the conversion of succinic acid to maleic anhydride were studied. These parameters included temperature, contact time, oxygen concentration, and water concentration. Also, the effect of time on-stream on catalyst performance was evaluated.

Temperature dependence was studied by changing the temperature of the middle zone of the furnace which actually enclosed the catalyst. Contact time was varied by changing the height of the bed of catalyst keeping the flow rates constant. A range of oxygen concentrations was achieved by controlling oxygen flow rate through the reactor by means of a mass flow controller. The effect of feed concentration was studied by using different succinic acid concentrations. Long time runs were conducted to study the possible deactivation of the catalysts with time. In order to keep all the reactions on an equal footing, a constant weight hour space velocity, defined as the mass of feed per mass of catalyst per hour (Robinson, 1989) was maintained throughout in all the runs.

3.3 Characterization of the catalysts

In order to characterize a catalyst sufficiently, it is necessary to determine the specific surface area, surface and bulk compositions, and the bulk crystal structure of the catalyst.

3.3.1 Surface area analysis:

The specific surface area, S_g (m^2gm^{-1}), is perhaps the singular most important particle parameter specified without regard to the type of surface. Measurement of surface area is based upon the principles of physical adsorption. Surface area of the catalysts is measured by nitrogen adsorption experiments done on a Micrometrics PulseChemisorb 2700 instrument. The Brunauer, Emmett, and Teller (BET) analysis (Robinson, 1989) is used to determine the actual surface area. This approach uses the BET equation shown below:

$$\frac{V}{V_M} = \frac{cp}{[p_0 - p] [1 + (c-1)p/p_0]} \quad (3.1)$$

Where,

p = pressure

p_0 = saturation pressure

V = volume adsorbed

V_M = monolayer volume

c = constant

The parameter c includes the heat of adsorption and liquefaction and is fairly constant for a given class of materials (like oxides and metals), with values below 100 (Robinson, 1989). The BET equation is valid only for low pressures, up to a value of 0.3 for p/p_0 . At higher

pressures, liquid condensation begins in the micropores and progresses through the mesopores as the pressure approaches the saturation pressure, i.e. $p/p_0 = 1.0$, at which point the equation breaks down.

Experimentally, it is impractical to measure V_M since it is valid in such a small region. However, a very practical method employed is to linearize the BET equation by rearranging the variables to obtain the following equation:

$$\frac{p}{V(p_0 - p)} = \frac{1}{V_M c} + \frac{(c-1)}{V_M c} (p/p_0) \quad (3.2)$$

This equation gives rise to linear plots whose slope and intercept can easily be measured. The value of V_M can be calculated as the inverse of the sum of the slope and the intercept. With this information, and knowing the weight of the sample used, the specific surface area (S) of the catalyst is easily determined by using equation (3.3).

$$S = V_M \cdot A \cdot N / M \quad (3.3)$$

where A = Avogadro's number

M = molar volume, and

N = area of each adsorbed gas molecule; for Nitrogen, $N = 16.2 \text{ nm}^2$

3.3.2 *X-Ray diffraction analysis:*

In X-ray diffraction, monochromatic x-rays are reflected from the sample with diffraction lines produced from the repetitive dimensions of crystal planes. Each crystal type gives a characteristic pattern, so that the position of the lines gives an idea of the particular phase of the compound that might be present in the sample (Richardson, 1989).

X-ray diffraction analysis was used in this work to determine the crystallinity of the catalyst. Once that was established, the exact crystalline phase of the material was determined by comparing the peaks obtained to the standard spectra available. Of special interest to this project was to determine whether a change in calcining conditions gave rise to any additional phases. Diffraction spectra of catalysts calcined at different temperatures were compared to determine the effect of calcining temperature on the catalysts.

The X-ray diffraction experiments were conducted on a Rigaku X-ray diffractometer having a rotating anode. Copper K α X-rays were generated by the machine which was used for the analysis.

3.3.3 *Bulk composition analysis:*

Elemental analysis of the catalyst was done in order to determine the bulk composition. Standard assays were employed to quantify percentages of iron, phosphorus, cerium, silicon, nitrogen, and any other elements that might be present. However, due to the inherent nature of the assays, it was not possible to determine the concentration of oxygen in the presence of metals. Bulk composition analyses of all catalysts were obtained from Galbraith Laboratories Inc., Tennessee.

Kjeldahl nitrogen was determined volumetrically. Decomposition was done in a Carius furnace. Steam distillation of the sample from the Kjeldahl flask was done after making it alkaline with excess of 50% NaOH. The liberated ammonia was trapped in saturated boric acid solution. Titration was carried out with 0.01N H₂SO₄ using methyl red-methylene blue indicator. Detection limit was 0.18 mg nitrogen. Quantitation limit was 0.3 mg nitrogen. Possible interferences were from N-N and N-O linkages.

Cerium was determined by inductively coupled plasma emission spectroscopy. Decomposition of the sample was done in a Carius furnace. Determination was by emission

at 413.77 nm. Detection limit was 1.6 ppm. Only spectral interferences were possible in this assay.

Silicon was determined by inductively coupled plasma emission spectroscopy. Decomposition was by fusion. Determination was by emission at 251.6 nm. Detection limit was 0.10 ppm.

Iron was determined by inductively coupled plasma emission spectroscopy. Decomposition was done either by wet digestion or by lithium metaborate fusion. Determination was by emission at 248.3 nm. Detection limit was 0.30 ppm.

Phosphorus was determined by plasma emission spectroscopy. Sample preparation involved decomposition by digesting in an acid mixture or by lithium metaborate fusion. Determination was by primary emission at 178.2 nm. Detection limit was 0.05 ppm.

3.3.4 *Surface composition analysis:*

The surface compositions of the catalysts is determined by using X-ray photoelectron spectroscopy (XPS). In XPS (or Electron Spectroscopy for Chemical Analysis, ESCA), use is made of the principle that a soft x-ray photon incident on a sample ejects any electrons with less binding energy. A sample is bombarded with monoenergetic photons like Al K α (1486.6 eV) or Mg K α (1253.6 eV), which ejects electrons from the core and valence shells in which the ionization potential, or binding energy, is less than the primary photon energy (Edmonds, 1980). These ejected electrons can be detected and counted to obtain a spectrum characteristic of the elements present in the sample. As sensitivity is possible only to depths of one to twenty layers, this technique gives information only on the weighted average surface composition of the sample. However, this is extremely desirable, since it is the surface of the catalyst that is the active part.

XPS data were obtained on a Perkin-Elmer Surface Science instrument equipped with a model 10-360 precision energy analyzer and an omnifocus small spot lens. X-rays were generated by an Al (1486.6 eV) anode operated at 15 kV and 20 mA. XPS binding energies were referenced to the C 1s line (284.6 eV) and were measured with a precision of ± 0.2 eV or better.

4. RESULTS AND DISCUSSIONS

4.1 Testing of commercial catalysts

Five commercially available catalysts were tested under different conditions in order to ascertain their suitability to the reaction being studied. These catalysts were obtained from United Catalyst Incorporated and were recommended by the manufacturers as proven dehydrogenation catalysts. Table 3.2 lists these catalysts and their constituents. Exact compositions are proprietary information.

Each of the catalyst was tested at two different temperatures. The temperatures chosen were 375 °C and 475 °C. Each run was conducted under the conditions specified below.

- a) contact time = 4 seconds,
- b) weight hourly space velocity (WHSV) = 0.8-0.9 gms reactant per gm of catalyst per hour,
- c) feed concentration = 40 grams per liter,
- d) oxygen to succinic acid mole ratio = 10:1, and
- e) time on-stream = 15 minutes.

The conversions and selectivities obtained are shown in Table 4.1. As is evident from the numbers in Table 4.1, the commercial catalysts showed little promise as a catalyst for the conversion of succinic acid to maleic anhydride. Although these catalysts gave conversions of over 90%, as evidenced by the relative size of the peaks on the NMR spectra, the selectivity to maleic acid was less than 1%. The poor selectivity was confirmed by the CO₂ electrode measurements which showed an extremely high percentage of CO₂

Table 4.1 Performance of commercial catalysts

CATALYST	TEMPERATURE (° C)	CONVERSION %	SELECTIVITY %
G-84 C	375	> 90	< 1
	475	> 90	< 1
G-65	375	> 90	< 1
	475	> 90	< 1
G-13	375	> 90	< 1
	475	> 90	< 1
G-22	375	> 90	< 1
	475	> 90	< 1
G-41	375	> 90	< 1
	475	> 90	< 1

formation during the reaction. It was thus evident that most of the reactants were being directly decarboxylated over the catalyst. The extremely small intensity of the peaks on the NMR spectrum made it impossible to measure the conversion with any greater accuracy than that reported.

The presence of a large amount of CO_2 is indicative of an acid catalyzed reaction. This can be explained on the basis of the metal oxides present in these catalysts. Metal oxides are active in the dissociation of steam at high temperatures. This leads to the dissociation of water and the subsequent formation of acid and base sites on the catalyst surface which significantly increases decarboxylation. Thus, it is unlikely that any acidic or basic catalyst will be suitable for the oxidative dehydrogenation reaction.

4.2 Testing of synthetic molybdenum oxide based catalysts

The three molybdenum oxide based catalysts synthesized in the laboratory were analyzed under the following conditions:

- a) contact time = 4 seconds,
- b) WHSV = 0.8 to 0.9 gm succinic acid per gram catalyst per hour,
- c) temperature = 475 °C,
- d) feed concentration = 40 gms per liter,
- e) oxygen to succinic acid ratio = 10:1, and
- f) total time on-stream = 30 minutes.

Table 4.2 shows the performance of these catalysts. All the molybdenum based catalysts yielded conversions of less than 10%; however, the selectivity towards maleic anhydride was always greater than 95%. This is confirmed by the NMR spectra obtained and by the CO_2 sensor which did not indicate the production of any measurable amount of carbon dioxide. The lack of CO_2 formation indicates that the postulated mechanism is operating and that, in this case, decarboxylation is not the predominant pathway.

Unfortunately, the molybdenum based catalysts possess an inherent low thermal stability which reduces their potential for commercial application to operating temperatures of less than about 400 °C. An irreversible phase change occurs at this temperature which makes it impossible to use these catalysts at higher temperatures, which is necessary to obtain higher conversions.

Based on these observations, it was decided to discontinue further testing of molybdenum based catalysts and to concentrate on those which would be better suited for commercial application.

4.3 Testing of synthetic iron phosphate based catalysts

Preliminary studies were done in order to test the ability of the iron phosphate based catalysts prepared in the laboratory to convert succinic acid to maleic anhydride. Initial testing revealed an improved conversion using catalysts promoted by cerium compared to those promoted by lanthanum under identical conditions. This observation resulted in limiting further testing to only those catalysts promoted by cerium.

4.3.1 *Effect of temperature on conversion:*

All the catalysts were tested for the conversion obtained and the selectivity towards maleic acid. Three different temperatures of 375 °C, 425 °C, and 475 °C were

Table 4.2 Performance of synthetic molybdenum based catalysts

CATALYST CONSTITUENTS	CONVERSION %	SELECTIVITY %
Mo, P, V, Cu, O	3	>95
Mo, P, V, W, O, H	9	>95
Mo, Ce, K, P, O	5	>95

tested. These temperatures were the broad ranges described in patent literature for the conversion of isobutyric acid to methacrylic acid (Daniel, 1983a,b,c etc.). The reactions were carried out under the following conditions:

- a) contact time = 4 seconds,
- b) WHSV = 0.8-0.9 grams reactant per gram of catalyst per hour,
- c) feed concentration = 40 grams per liter,
- d) oxygen to succinic acid mole ratio = 10:1, and
- e) total time on-stream = 30 minutes.

Figure 4.1 shows the results obtained for these catalysts. The results show a very promising trend for the iron phosphate based catalysts. From the results obtained, it is evident that temperature is a very important variable in the performance of the catalysts. For all the catalysts, at 375 °C, the conversions obtained were between 16% and 33%; whereas, at 475 °C, the conversions obtained were between 49% and 59%. This establishes that a higher temperature is more favorable for the reaction within the chosen range.

Also, the selectivities obtained were all greater than 95%. Almost no production of carbon dioxide or any other by-products was observed. Less than 5% of succinic acid feed was converted to acrylic acid and CO₂. This high selectivity obtained with the iron phosphate based catalysts is more than that achieved for the analogous reaction of isobutyric to methacrylic acid reported in patent literature.

These results conclusively prove that succinic acid can be converted to maleic anhydride using the iron phosphate based catalysts. The high selectivity obtained is believed to be a consequence of the inherent stability of the five membered ring of succinic anhydride. The absence of any free succinic acid sites offers little opportunity for decarboxylation and subsequent production of carbon dioxide to occur.

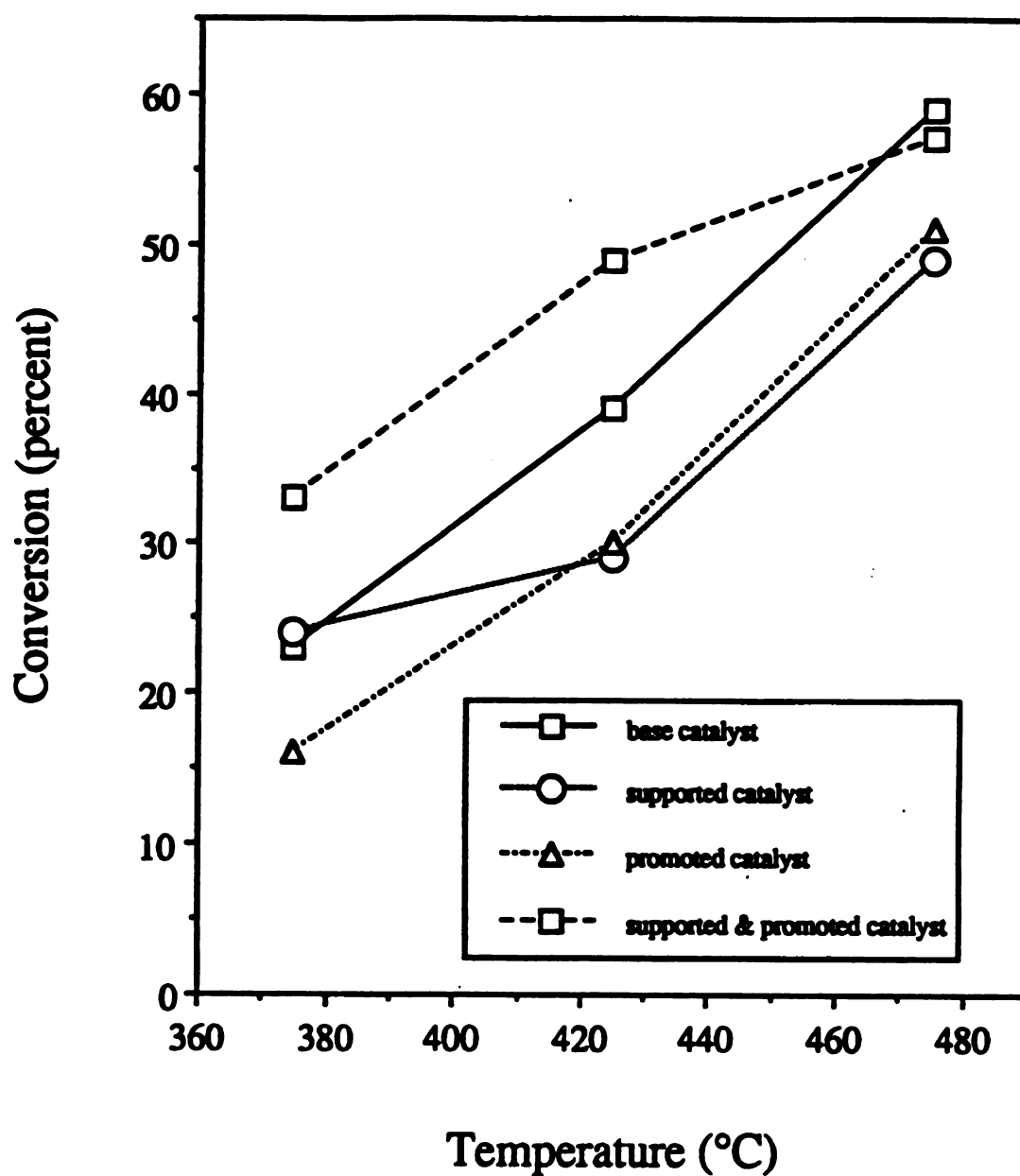


Figure 4.1 Effect of temperature on the conversion of succinic acid to maleic acid using iron phosphate catalysts under the following conditions: a) contact time = 4 s, b) WHSV = 0.8-0.9 gm feed/gm catalyst/hr, c) feed concentration = 40 g/l, d) oxygen to feed mol ratio = 10:1, and e) time on-stream = 30 minutes

Based on these results, it was decided to conduct further studies on these four catalysts only at 475 °C in order to optimize other conditions for the best operation of the reactor.

4.3.2 *Effect of contact time on conversion:*

The effect of contact time on the conversion of succinic acid to maleic acid over two iron phosphate based catalysts was studied in order to establish the optimum contact time to be used. The experiments were carried out under the following reaction conditions:

- a) Feed concentration = 40 g/L,
- b) WHSV= 0.8 to 0.9 grams succinic acid per gram of catalyst per hour,
- c) Temperature = 475 °C,
- d) Oxygen to succinic acid mole ratio = 25:1, and
- e) Total time on-stream = 15 minutes.

The results of the experiments are shown in Figure 4.2. For both the pure base catalyst and the base catalyst with support and promoter, the optimum contact time was determined to be 4 seconds. All of the iron phosphate catalysts tested showed approximately 15% less conversion at a contact time of 2 seconds as compared to a contact time of 4 seconds. A contact time of 6 seconds shows virtually no increase in the conversions obtained. It is to be noted that under all conditions, the selectivities obtained for the iron phosphate based catalysts were higher than 95%.

This is an indication that equilibrium is achieved in four seconds. Based on this, it was decided to conduct all future experiments at a contact time of 4 seconds.

4.3.3 *Effect of feed concentration on conversion:*

In a typical fermentation broth, the concentration can be expected to fluctuate somewhat depending on the the conditions in the fermenter and on the efficiency of

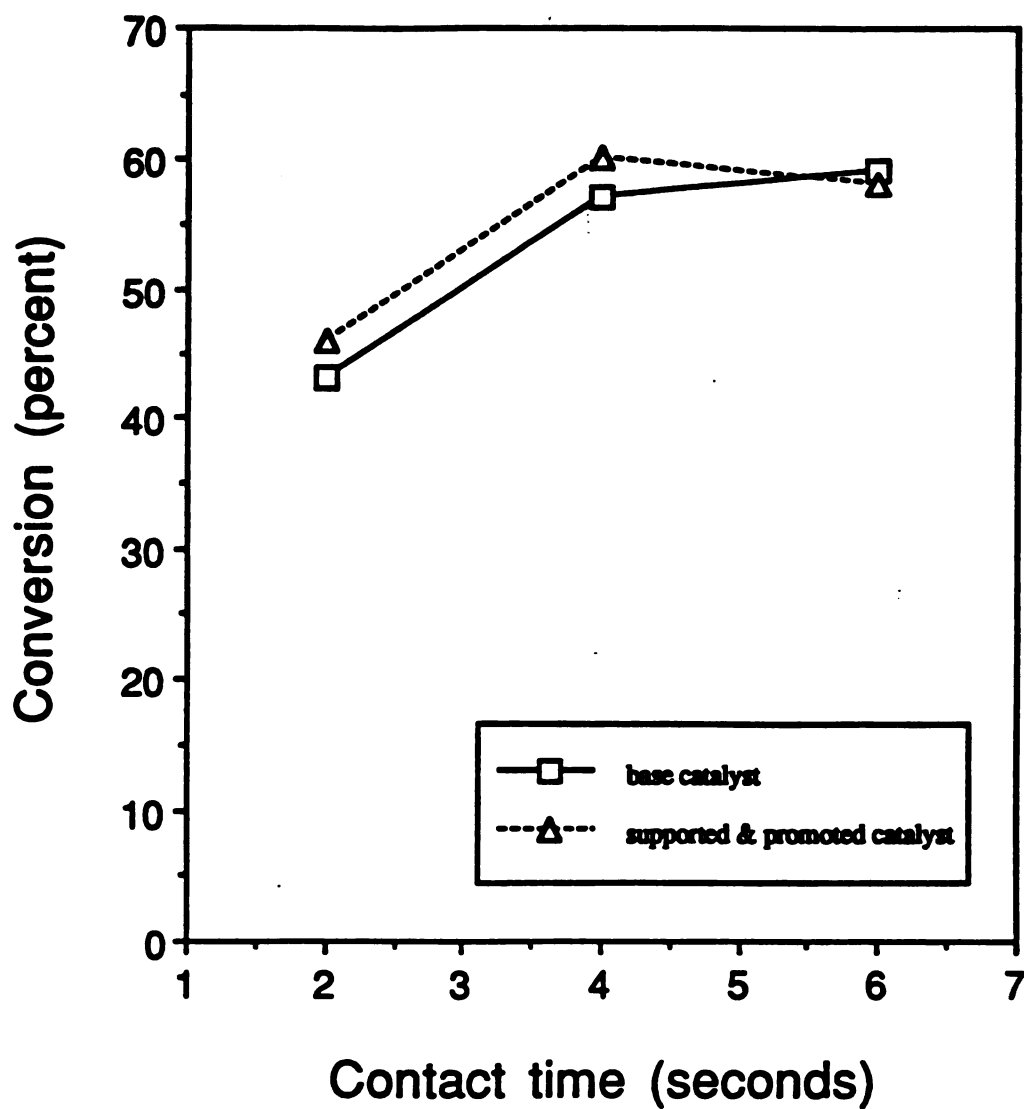


Figure 4.2 Effect of contact time on the conversion of succinic acid to maleic acid using iron phosphate catalysts under the following conditions: a) temperature = 475 °C, b) WHSV = 0.8-0.9 gm feed/gm catalyst/hr, c) feed concentration = 40 g/l, d) oxygen to feed mol ratio = 25:1, and e) time on-stream = 15 minutes

separation. This implies that the concentration of feed obtained can vary in concentration. It is thus imperative to study the effect of feed concentration on the catalyst performance.

The effect of the feed concentration on conversion and selectivity was tested by using two concentrations of 40 g/L and 80 g/L. The results of the experiments are shown in Figure 4.3. All the experiments were carried out under the following reaction conditions:

- a) Contact time = 4 seconds,
- b) WHSV= 0.8 to 0.9 grams succinic acid per gram of catalyst per hour,
- c) Temperature = 475 °C,
- d) Oxygen to succinic acid mole ratio = 25:1, and
- e) Total time on-stream = 15 minutes.

From the results obtained, it is evident that the catalysts tested performed equally well even when the feed concentration was doubled from 40 g/L to 80 g/L. Again, selectivities obtained were greater than 95%. This indicates the versatility of the catalyst towards the range of feed concentrations expected from a typical fermentation product.

4.3.4 *Effect of oxygen concentration on conversion:*

The amount and purity of oxygen required for the oxidative dehydrogenation reaction to take place is an important parameter since the cost of oxygen will be a major factor in the economics of the process. Experiments were carried out with two catalysts varying the relative concentrations of oxygen to the feed. The experiments were conducted under the following conditions:

- a) Contact time = 4 seconds,
- b) WHSV= 0.8 to 0.9 grams succinic acid per gram of catalyst per hour,
- c) Total time on-stream = 15 minutes, and
- d) Feed concentration = 40 g/L.

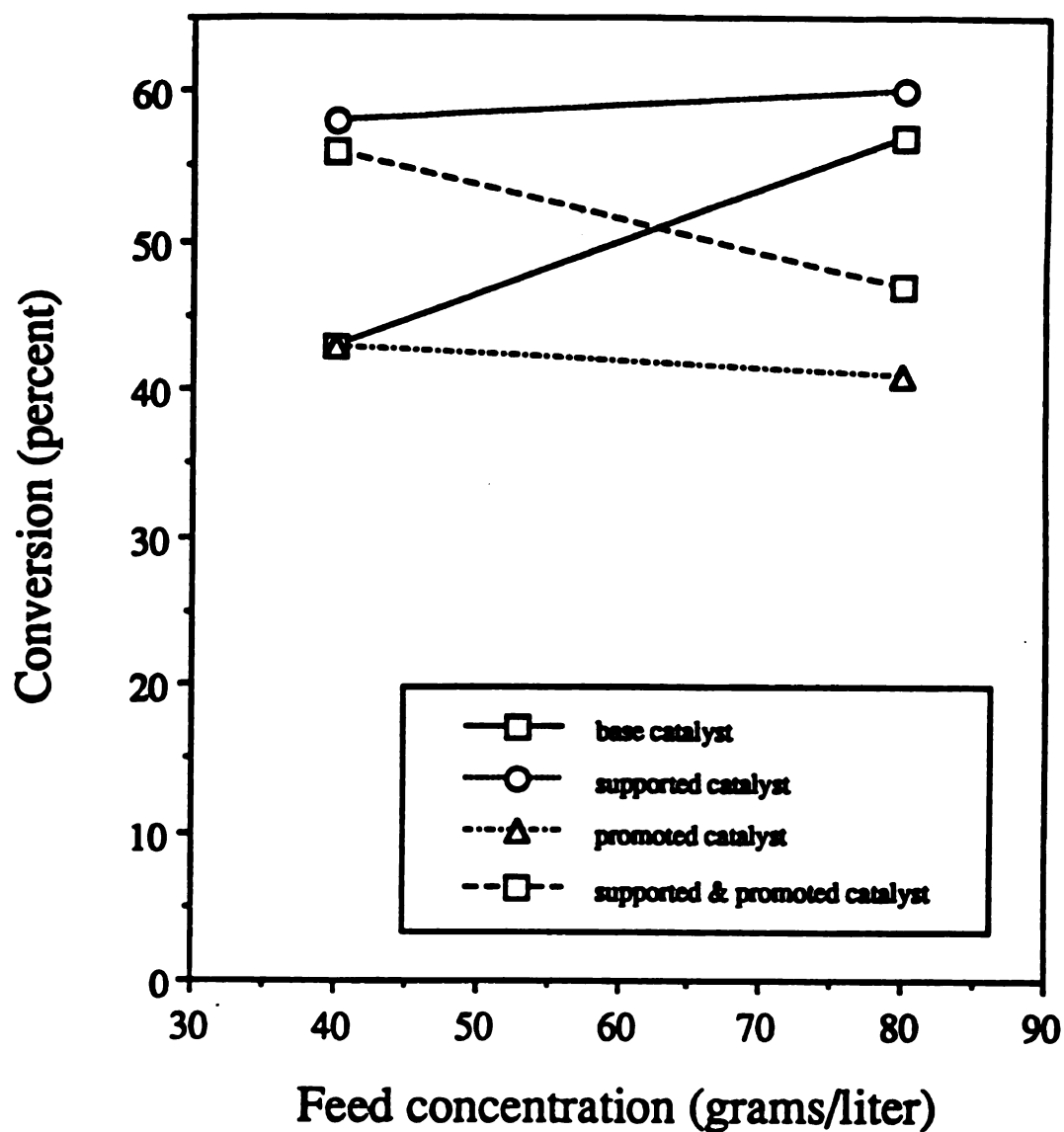


Figure 4.3 Effect of feed concentration on the conversion of succinic acid to maleic acid using iron phosphate catalysts under the following conditions: a) contact time = 4 s, b) WHSV = 0.8-0.9 gm feed/gm catalyst/hr, c) temperature = 475 °C, d) oxygen to feed mol ratio = 25:1, and e) time on-stream = 15 minutes

The results of the experiments are shown in Figure 4.4. In all experiments, the selectivities obtained were over 95%. The results indicate that when the mole ratio of oxygen to succinic acid was greater than 10:1, there was no substantial increase in the conversions obtained. If the proposed mechanism for oxidative dehydrogenation was working, the total oxygen requirement for conversion of succinic acid to maleic anhydride would be stoichiometric with respect to succinic acid. In all the experiments conducted, the oxygen concentration used was always above at least ten times the minimum required; so the result obtained, i.e., no change in conversion with increase in oxygen concentration is only to be expected and further substantiates the proposed mechanism. This low oxygen requirement strongly suggests that pure oxygen is not required for large scale production and that air should be an adequate source of oxygen, thereby reducing the operating cost substantially.

4.3.5 *Effect of time on-stream on conversion:*

Experiments were conducted on two catalysts to test their performance after different time intervals. This information is of interest because it would determine whether the catalysts need to be regenerated after a certain amount of time. The experiments were carried out under the following reaction conditions:

- a) Contact time = 4 seconds,
- b) WHSV = 0.8 to 0.9 grams succinic acid per gram of catalyst per hour,
- c) Temperature = 475 °C,
- d) Oxygen to succinic acid mole ratio = 25:1, and
- e) Feed concentration = 40 g/L.

The effect of time on-stream on catalyst performance is shown in Figure 4.5. Selectivities achieved were greater than 95%. From the results, it is seen that the base iron phosphate catalyst shows a slight decrease in conversion with time; whereas, the catalyst promoted with cerium and supported with silica shows a slight increase in conversion after

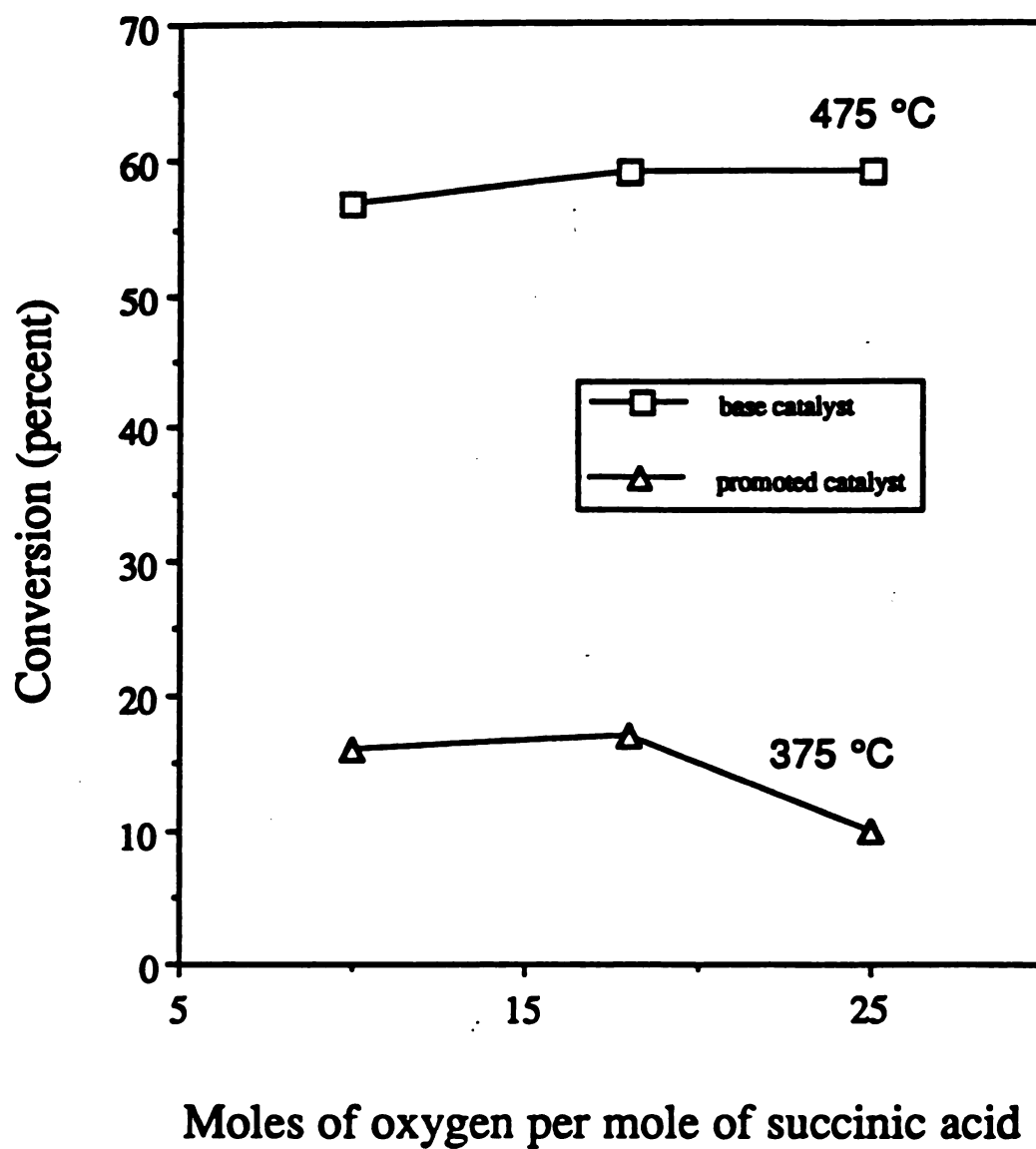


Figure 4.4 Effect of oxygen concentration on the conversion of succinic acid to maleic acid using iron phosphate catalysts under the following conditions: a) contact time = 4 s, b) WHSV = 0.8-0.9 gm feed/gm catalyst/hr, c) feed concentration = 40 g/l, and d) time on-stream = 15 minutes

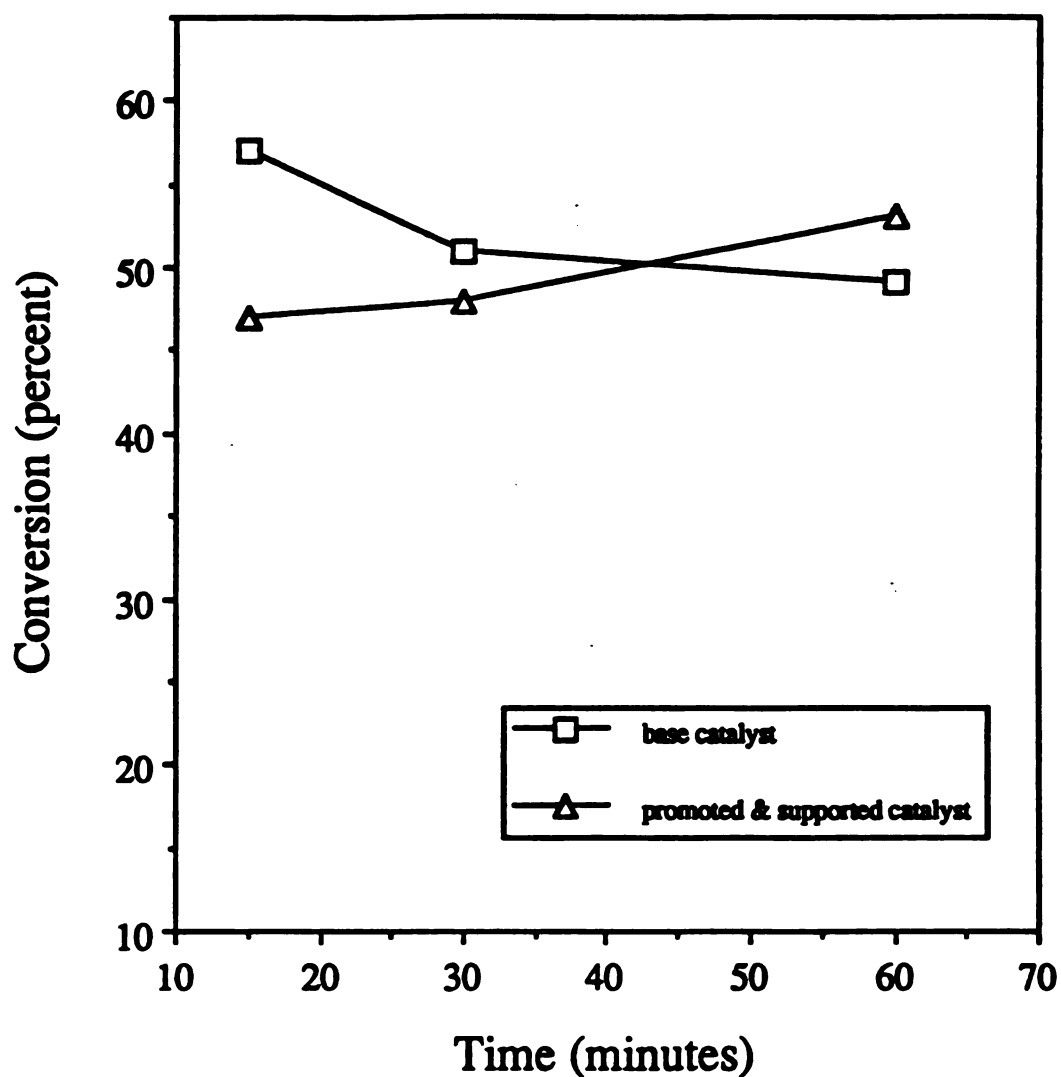


Figure 4.5 Effect of time on-stream on the conversion of succinic acid to maleic acid using iron phosphate catalysts under the following conditions: a) contact time = 4 s, b) WHSV = 0.8-0.9 gm feed/gm catalyst/hr, c) temperature = 475 °C, d) feed concentration = 40 g/l, and e) oxygen to feed mol ratio = 25:1

60 minutes. However, there is no indication of any significant change in the catalyst performance with time. Although the runs need to be conducted for a longer length of time, indications are that catalyst poisoning and regeneration are not significant problems for these catalysts.

4.4 Results of characterization experiments

To characterize the catalysts under study, it was decided to find the surface area of each of the catalysts, to determine the bulk and surface compositions and to try and determine the crystal structure information of each of the catalysts. The techniques used were physisorption, X-ray diffraction and X-ray photoelectron spectroscopy.

4.4.1 Surface area measurements:

As discussed in the previous chapter, the linearized BET relation (eq.3.2) reproduced below, was used to calculate the surface areas of the catalysts. Multipoint analysis was used to ensure better accuracy. Nitrogen partial pressures of 5, 10 and 20 percent were chosen.

$$\frac{p}{V(p_o - p)} = \frac{1}{V_M c} + \frac{(c-1)}{V_M c} (p/p_o) \quad (3.2)$$

A graph of $p/(V(p_o - p))$ vs. p/p_o gives a straight line with a slope of $(c-1)/(V_M c)$ and an intercept of $1/(V_M c)$. As described in the previous chapter, the slope and intercept can be utilized to give the surface area of the catalyst in $m^2 gm^{-1}$ using equation 3.3.

Figure 4.6 shows a typical BET plot for a base iron phosphate catalyst with a silica support and with cerium as a promoter. The slope and the intercept together give the surface area by using equation 3.3. Table 4.3 shows the calculated surface area for each of the four catalysts.

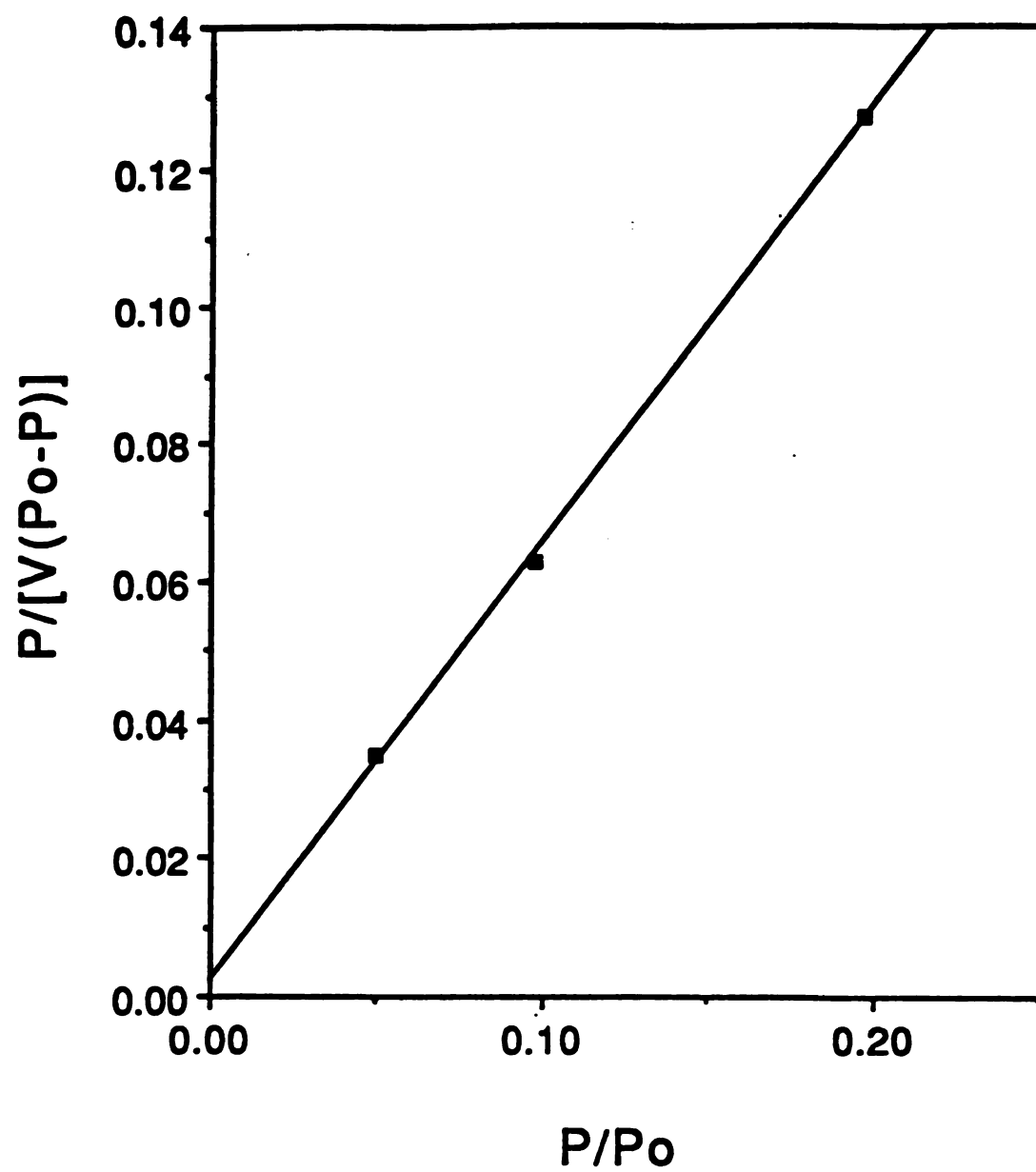


Figure 4.6 Typical BET plot for a supported and promoted iron phosphate catalyst

Table 4.3 Surface areas of catalysts

CATALYST	SURFACE AREA, m ² /gm
Base iron phosphate	2.66
Base iron phosphate+LUDOX® HS 40%	2.73
Base iron phosphate+Ce promoter	3.20
Base iron phosphate+Ce+LUDOX® HS 40%	6.38

It is to be noted that the surface area of all the iron phosphate catalysts are extremely low, less than 10 m²/gm. Even the catalyst containing a silica support did not show an increase in the surface area. This shows that it is not possible to make catalysts with high surface areas.

4.4.2 Bulk compositions:

Bulk compositions of the four iron based catalysts were obtained by analyses conducted at Galbraith Laboratories, Inc. The assays used are described in the previous chapter. The only drawback of the assay used is that it is impossible to obtain the concentration of oxygen in the presence of other metals like iron.

Table 4.4 gives the bulk composition of the catalysts. As expected, the proportions of iron and phosphorus are approximately the same, whereas the amount of nitrogen is quite low. This indicates that the catalyst preparation reaction went almost to completion and that all the nitrates were substituted by phosphates forming nitric acid. Since no other elements were introduced initially, it is reasonable to assume that the remaining percentage is all oxygen.

Table 4.4 Bulk molar compositions of the catalysts

CATALYST	IRON %	PHOSPHORUS %	NITROGEN %	CERIUM %	SILICON %	OXYGEN %
Base iron phosphate	26.82	25.47	< 0.5	-	-	~ 47.21
Base iron phosphate + LUDOX® HS 40%	21.19	23.93	< 0.1	-	6.26	~ 48.51
Base iron phosphate + Ce promoter	29.13	21.85	< 0.1	1.03	-	~ 47.89
Base iron phosphate + Ce+LUDOX® HS 40%	22.23	21.04	< 0.11	2.52	8.02	~ 46.08

4.4.3 *Surface compositions:*

Surface compositions were measured using X-ray photoelectron spectroscopy. XPS data were obtained on a Perkin-Elmer Surface Science instrument equipped with a model 10-360 precision energy analyzer and an omnifocus small spot lens. X-rays were generated by an Al (1486.6 eV) anode operated at 15 kV and 20 mA. XPS binding energies were referenced to the C 1s line (284.6 eV) and were measured with a precision of ± 0.2 eV or better. The samples were outgassed at 400 °C for 24 hours to remove any surface moisture accumulated during storage.

Table 4.5 gives the relative surface compositions of each of the four catalysts relative to the amount of iron on the surface. It is to be noted that in almost all cases, the surface composition is quite different from the bulk composition. The concentration of iron sites on the surface is much less as compared to the other elements. The concentration of phosphorus atoms is at least five times greater than that of iron at the surface, whereas the concentration of oxygen is more than ten times that of iron. It is to be noted that in all catalysts, there is a significant amount of carbon observed. This is carbon adsorbed onto the surface from hydrocarbons present in air, a general contaminant in XPS. The fact that surface compositions differ so widely from the bulk compositions suggests that either a better control needs to be implemented during the preparation of the catalyst in order to ensure a homogeneous distribution of all the elements throughout the catalyst, or that it is simply not possible for iron to be in larger quantities on the surface.

4.4.4 *Bulk crystal structure determination:*

X-ray diffraction techniques were used to try and identify the various crystal phases believed to be present in the bulk catalyst. Although the catalysts proved to be extremely crystalline, no single phase was uniquely present in any of the catalysts. As the spectra obtained show, a mixture of phases is present in all catalysts.

Table 4.5 Surface molar compositions of the catalysts relative to iron content

CATALYST	IRON	PHOSPHORUS	NITROGEN	CERIUM	SILICON	OXYGEN	CARBON
Base iron phosphate	1	8	0.53	-	-	18	4.5
Base iron phosphate + LUDOX® HS 40%	1	7	0.58	-	4.7	25	6.4
Base iron phosphate + Ce promoter	1	11	0.91	0.27	-	32	9.2
Base iron phosphate + Ce+LUDOX® HS 40%	1	5	0.34	0.04	1.2	13	4.5

X-ray diffraction patterns were obtained using a Rigaku diffractometer equipped with a rotating anode and using Cu-K α radiation. An operating voltage of 45kV and an operating current of 100mA was used. The slit sizes used were: DS = 0.5, SS = 0.5, RS = 0.3, and RSm = 0.45. X-ray diffraction spectra were obtained for all the four catalysts calcined at two different conditions. One set was calcined at 110 °C while the other was calcined at 500 °C as described earlier. Figure 4.7a shows the diffraction spectrum for a catalyst calcined at 110 °C and Figure 4.7b shows the same catalyst calcined at 500 °C. An inspection of the two indicates that at a higher temperature, although the degree of crystallinity does not change much, new phases are created which replace existing crystallographic phases. This indicates that calcination temperature is an important parameter in the preparation of the catalyst. The diffraction spectra for all the other catalysts are included in Appendix B.

An attempt was made to identify the various crystallographic phases present by comparing the d-spacings obtained from the spectrum to those of known crystallographic phases available in literature. The one phase common in all the catalysts is Fe(PO₃)₃; Iron (III) metaphosphate. Other forms of Fe(PO₃)₃ are also present along with a number of as yet unidentified phases. A study of these diffraction spectra is evidently important as it will provide a yardstick to check the reproducibility of future catalyst preparations.

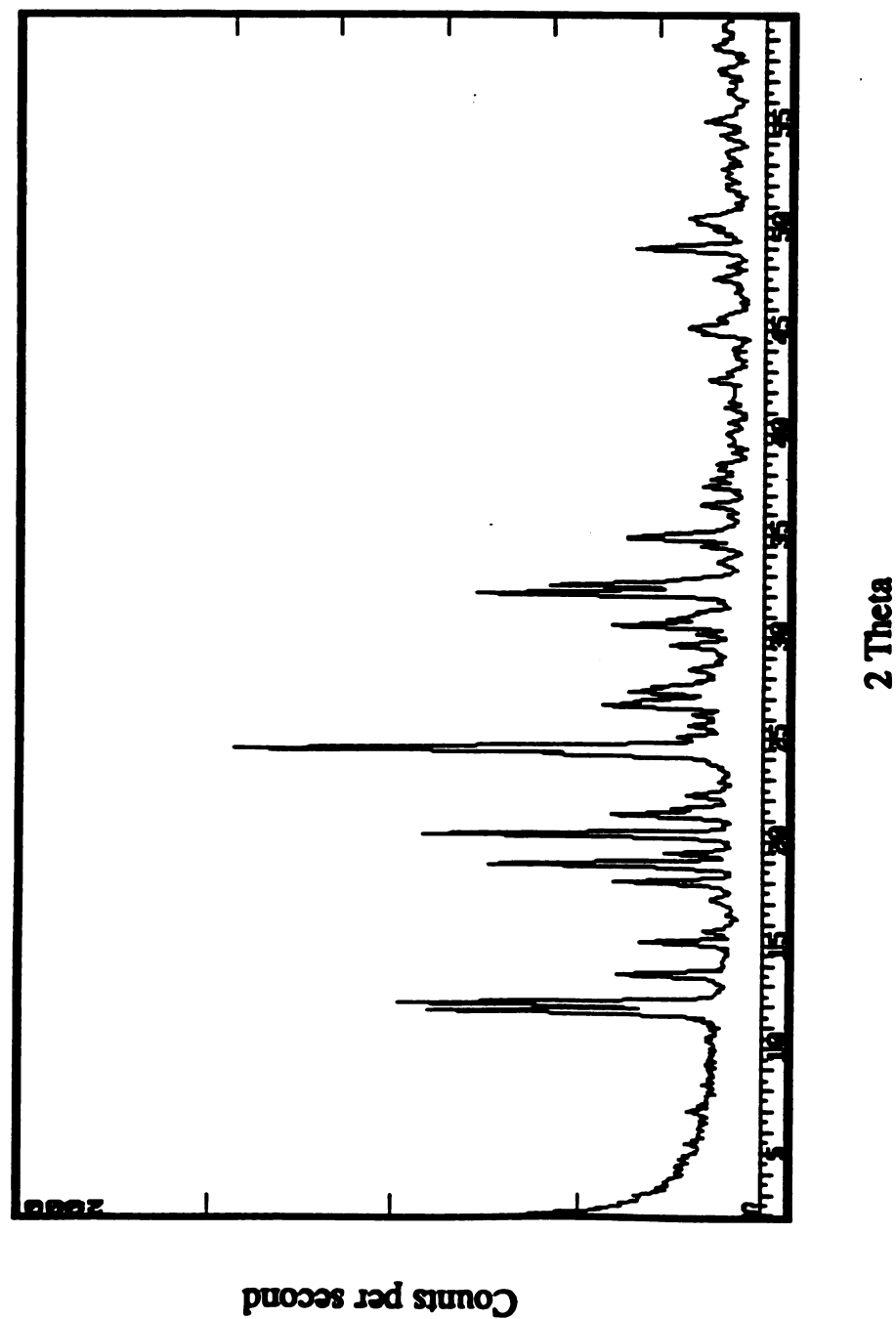


Figure 4.7a X-Ray diffraction spectrum of an iron phosphate catalyst, calcined at 110 °C

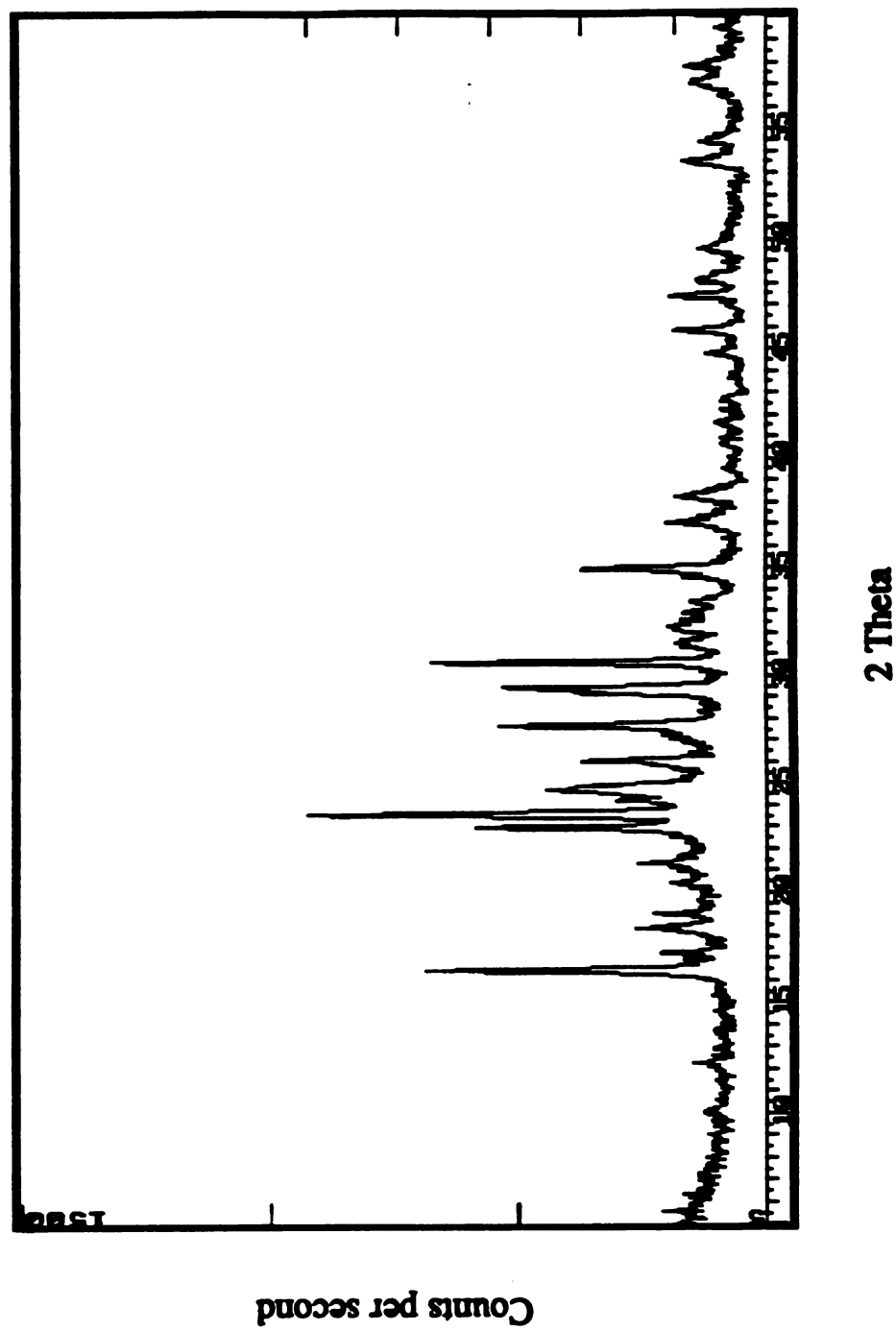


Figure 4.7b X-Ray diffraction spectrum of an iron phosphate catalyst, calcined at 500 °C

5. CONCLUSIONS

Conventional commercial dehydrogenation catalysts offer little promise in achieving the conversion of succinic acid to maleic anhydride under oxidative dehydrogenation conditions. The selectivities achieved are extremely poor which makes these catalysts non-competitors in the attempt to find a catalyst suited for commercial production.

This work demonstrates that unlike the commercial catalysts, the molybdenum based catalysts show a high degree of selectivity, although the conversions obtained are very low; none of them exhibiting a conversion greater than 10%. Also, the inherent instability of these catalysts at higher temperatures render them unsuitable for use at temperatures in excess of 400 °C, which may be necessary.

The results obtained with the iron phosphate catalysts are very promising. Experiments were conducted using the base iron phosphate catalyst, the base catalyst promoted by cerium, the base catalyst with a silica support and the base catalyst with both the promoter and the support. In all cases a conversion of at least 40% has been achieved. High selectivities (>95%) were also achieved which makes these catalysts extremely viable for the commercial production of maleic anhydride from fermentation feedstocks.

The high conversions and selectivities obtained are attributed to the stability of the five membered ring structure of succinic anhydride. This stable structure minimizes the opportunity for decarboxylation to occur.

From the experiments conducted, the iron phosphate based catalysts indicate high conversions and selectivities even in the presence of copious amounts of water. Also, it is evident that large amounts of pure oxygen are not required for the reaction to take place and that on an industrial scale, atmospheric air should provide sufficient oxygen for the reaction, thus favoring the economics of the entire process.

The experiments also indicate that the base iron phosphate catalysts achieve as good conversions and selectivities as the ones supported by silica, indicating that the support does not play a significant role. There seems to be an advantage in using the cerium promoter but further studies are required for confirmation.

Characterization experiments were conducted in order to determine the physical attributes of the iron phosphate based catalysts. The surface area of the catalysts were measured which indicates the extremely low active surface area available for the reaction, on the order of less than $10 \text{ m}^2\text{gm}^{-1}$. Bulk composition analyses were conducted which were then compared with the surface composition data obtained by XPS. In all cases, the surface composition was quite different compared to the bulk compositions. X-ray diffraction experiments were conducted in order to determine the crystalline phases present under different calcining conditions. New phases were created when the catalysts were calcined at a higher temperature of 500°C . A mixture of different phases was present in each catalyst. Although some of these phases could be identified by comparing with standard known phases, there were some new phases present which could not be identified.

6. RECOMMENDATIONS FOR FUTURE WORK

It has been established in this work that the iron phosphates catalysts are indeed suitable for the production of maleic anhydride from succinic acid. Certain other operating parameters like temperature, contact time etc. have also been optimized. However, for the catalytic process to be adapted to industry, it is also necessary to optimize the conditions under which the catalysts are prepared and characterized as well as all the design and operating parameters in the overall process.

Out of the four iron phosphate based catalysts tested in this work, it was not conclusively proven which was the best suited for the reaction under study. Additional experiments will have to be carried out to determine the most suitable catalyst. The conversions obtained using a more expensive promoted catalyst have to be evaluated vis-a-vis the conversions obtained from an unpromoted catalyst to decide whether the increase in cost is justified by an increase in product yield. Other promoters like cesium will have to be tested instead of cerium to see if a higher conversion can be achieved. At present, the use of a silica support does not indicate any increased performance compared to an unsupported but promoted catalyst.

Once the catalyst that gives the highest conversions and selectivities is determined, it is essential to find out the rate equation for the catalyzed reaction. Simple kinetic experiments will be needed to determine the rate equation and the constants therein. The rate equation may turn out to be of a complex order, but in any case, it will provide valuable information on the theoretical conversions attainable under different conditions.

The particle size and shape of the catalyst to be used is an important parameter to be studied. These decide the extent of diffusion and mass transfer resistances on the surface and also the pressure drop across the bed of catalysts.

Certain conditions during the synthesis of the catalysts need to be optimized. Although the conditions used in this work appear to be reasonably well suited, further catalyst preparations under different conditions will be necessary to determine the best possible set of conditions. Of specific interest will be the conditions under which the catalysts are calcined. It has been established that calcining at a higher temperature results in a change in the crystal structure of the catalyst. Further experiments on the same lines will have to be done to determine the most favorable crystal structure of the catalyst.

Bulk elemental analysis as well as surface composition analysis using XPS, as was done in this work, will be an invaluable tool providing direct information on the distribution of the various elements throughout the catalyst material.

Further characterization work will have to be done in order to ensure the reproducibility of the catalyst synthesis. Powder X-ray diffraction experiments will indicate whether every crystal phase is reproduced each time or not. These experiments can also determine the metal crystal sites as well as identify any contaminant phase in spent catalysts.

The technique of Mössbauer (or nuclear gamma resonance) spectroscopy provides information on such parameters as isomer shift, quadrupole splitting and magnetic hyperfine splitting. These parameters allow a detailed analysis of the chemical state of any desired atoms within a material and as such will be utilized to provide a more complete picture of the iron phosphate catalysts. For example, the oxidation states of iron before and after the catalytic reaction can be determined. Mössbauer spectroscopy can also provide a

viable means of investigating the exact role of promoters. Jones (1980) has discussed some of these applications with iron oxide catalysts as an example.

Phosphorus NMR (nuclear magnetic resonance) can also provide a very accurate measure of the concentration of phosphorus on the surface and in the bulk catalyst.

Although catalytic activity, selectivity and the deactivation rate are important criteria for developing and evaluating commercial catalysts, mechanical properties such as catalyst stability, attrition resistance and crushing strength are just as important (Bertolacini, 1989). For this reason it is essential that the catalysts under study be tested for single pellet and bulk crushing strengths. The exact form in which the catalysts are to be manufactured, that is, whether they should be extruded, pelletized, etc. has to be decided upon. Also, if pellets are to be made, it has to be decided if the pellets will be spherical or cylindrical. Standardized procedures need to be developed for the industrial scale manufacture of the catalysts.

As discussed previously, the ultimate aim of this project is to produce maleic anhydride from a *fermentation derived* succinic acid. All the experiments carried out in this study utilized pure succinic acid procured from the market. It is therefore necessary to test these catalysts on succinic acid obtained directly from a fermentation broth. The broth will contain certain impurities like amino acids, other proteins and acetic acid, and the performance of the catalyst in the presence of these impurities will have to be evaluated. In this work, feed concentrations of 40 g/L and 80 g/L were tested. These are the expected range of concentrations in a typical fermentation broth. Of special interest will be the performance of the catalyst at much higher concentrations. If significantly higher yields are achieved, the ability of these catalysts to perform at higher concentrations may provide an economic advantage in which case the feed will have to be concentrated before being fed into the reactor.

Atmospheric air has to be tested to see if it can be used instead of pure oxygen in order to cut costs. The feed to air ratio to be used has to be optimized.

It is also essential to determine the catalyst life without the need for regeneration. In this work, the catalysts showed virtually no deactivation at the end of one hour. However, further tests will have to be carried out to determine the lifetime of the catalyst in a continuous operation of the reactor. Once that is known, tests will have to be carried out to determine if the catalysts can be regenerated to their original state. Reoxidation and steam treatment will be the two primary methods to regenerate the catalysts.

Finally, the reactor design itself has to be optimized. While a fixed bed operation seems to work reasonably well, it might be more advantageous to use a fluidized bed, especially if frequent regeneration is required during a continuous operation. In that case a parallel can be drawn from the fluidized catalytic cracking (FCC) column widely used in the petroleum industry, wherein regular regeneration is practiced in a continuous process. A large pilot scale reactor will be required to make a realistic economic survey of the overall process. An economically favorable survey will be an indication of an optimum reactor design which has to integrate the fermentation process to produce succinic acid and the catalytic conversion technology developed in this work to convert the succinic acid to maleic anhydride.

APPENDICES

APPENDIX A

LABORATORY SYNTHESIS PROCEDURE FOR THE CATALYSTS

A. Iron phosphate based catalysts:

1. Iron phosphate

The base iron phosphate catalyst was prepared by dissolving 48.5 grams of $\text{Fe}(\text{NO}_3)_3 \cdot 9\text{H}_2\text{O}$ (iron nitrate nonahydrate) and 15 ml of H_3PO_4 (85%) in 120 ml of water. The solution was refluxed with constant stirring and heating; after 2 hours of refluxing, a creamish slurry was formed. Refluxing was carried on for about 20 hours, after which the slurry was distilled to form a thick paste. The paste was dried in an oven at 110 °C for about 24 hours. The catalyst was calcined at 450 °C for 6 hours in a forced air oven. A second calcination was performed in a quartz reactor tube at 500 °C for 2 hours with an oxygen flow rate of 10 ml/min and a nitrogen flow rate of 10 ml/min.

2. Iron phosphate with silica support

The base iron phosphate catalyst with a silica support was prepared exactly as in preparation 1, but with the addition of 10 ml of Ludox[®] HS 40% to the aqueous solution. The catalyst was calcined in a similar fashion.

3. Cerium promoted iron phosphate

The base iron phosphate catalyst with a promoter (5% cerium) was prepared exactly as in preparation 1, but with the addition of 2.5 grams of $\text{Ce}(\text{NO}_3)_3 \cdot 6\text{H}_2\text{O}$ (cerium

nitrate hexahydrate) to the aqueous solution. The catalyst was calcined in a similar fashion.

4 . Lanthanum promoted iron phosphate

The base iron phosphate catalyst with a lanthanum promoter was prepared exactly as in preparation 1, but with the addition of 9.9 grams of lanthanum pentaoxide to the aqueous solution. The catalyst was calcined in a similar fashion.

5 . Cerium promoted iron phosphate catalyst supported on silica

The base iron phosphate catalyst with a promoter (5 % cerium) and a silica support was prepared exactly as in preparation 1, but with the addition of 2.5 grams of $\text{Ce}(\text{NO}_3)_3 \cdot 6\text{H}_2\text{O}$ and 10 ml of Ludox[®] HS 40% to the aqueous solution. The catalyst was calcined in a similar fashion.

6 . Lanthanum promoted iron phosphate catalyst supported on silica

The base iron phosphate catalyst with a lanthanum promoter and a silica support was prepared exactly as in preparation 1, but with the addition of 2.5 grams of lanthanum pentaoxide and 10 ml of Ludox[®] HS 40% to the aqueous solution. The catalyst was calcined in a similar fashion.

B. Molybdenum oxide based catalysts:

- 7 . The first catalyst was prepared by adding 0.71 ml of H_3PO_4 (85%), 1.17 grams of NH_4VO_3 , 19.5 grams of $(\text{NH}_4)_2\text{Mo}_2\text{O}_7$, and 0.48 grams of $\text{Cu}(\text{NO}_3)_2 \cdot 2.5\text{H}_2\text{O}$ to 300 ml of water. A fine suspension was formed. The water was evaporated off to form a thick paste. The paste was dried in air in an oven for 12 hours at 155 °C. The catalyst was calcined at 400 °C in a forced air oven for six hours. A second calcination was performed in a quartz reactor tube at 400 °C for 2 hours with an oxygen flow rate of 10 ml/min and a nitrogen flow rate of 10 ml/min.

The resulting catalyst was composed of molybdenum, phosphorus, vanadium, copper, and oxygen.

8. The second molybdenum oxide based catalyst was prepared by adding 1.6 ml of H_3PO_4 (85%), 30 grams of MoO_3 , 2.1 grams of V_2O_5 , and 10.7 grams of WO_3 to 200 ml of distilled water. The suspension formed was refluxed for 72 hours. It was filtered after being cooled to room temperature. The filtrate was evaporated to dryness at 120°C , and dried in an oven at 115°C for 16 hours. The catalyst was calcined at 400°C in a forced air oven for six hours. A second calcination was performed in a quartz reactor tube at 400°C for 2 hours with an oxygen flow rate of 10 ml/min and a nitrogen flow rate of 10 ml/min.

The resulting catalyst was composed of molybdenum, phosphorus, vanadium, tungsten, oxygen, and hydrogen.

9. The third molybdenum based catalyst was prepared by adding 27 grams of $(\text{NH}_4)_6\text{Mo}_7\text{O}_{24}\cdot 4\text{H}_2\text{O}$, 8.1 grams of $(\text{NH}_4)_2\text{Ce}(\text{NO}_3)_6$, 1.73 grams of KOH, 3.2 ml of H_3PO_4 (85%), and 30 ml of concentrated HCl to 30 ml of distilled water. The resulting slurry was heated at 125°C to a thick paste. The paste was dried in an oven at 115°C for 18 hours. The catalyst was calcined at 400°C in a forced air oven for six hours. A second calcination was performed in a quartz reactor tube at 400°C for 2 hours with an oxygen flow rate of 10 ml/min and a nitrogen flow rate of 10 ml/min.

The resulting catalyst was composed of molybdenum, cerium, potassium, phosphorus, and oxygen.

APPENDIX B

X-RAY DIFFRACTION SPECTRA OF THE CATALYSTS

The X-ray diffraction spectra of the base iron phosphate catalyst calcined at 110 °C and at 500 °C were shown in Chapter 4. The diffraction spectra for all the other catalysts are compiled in the following pages.

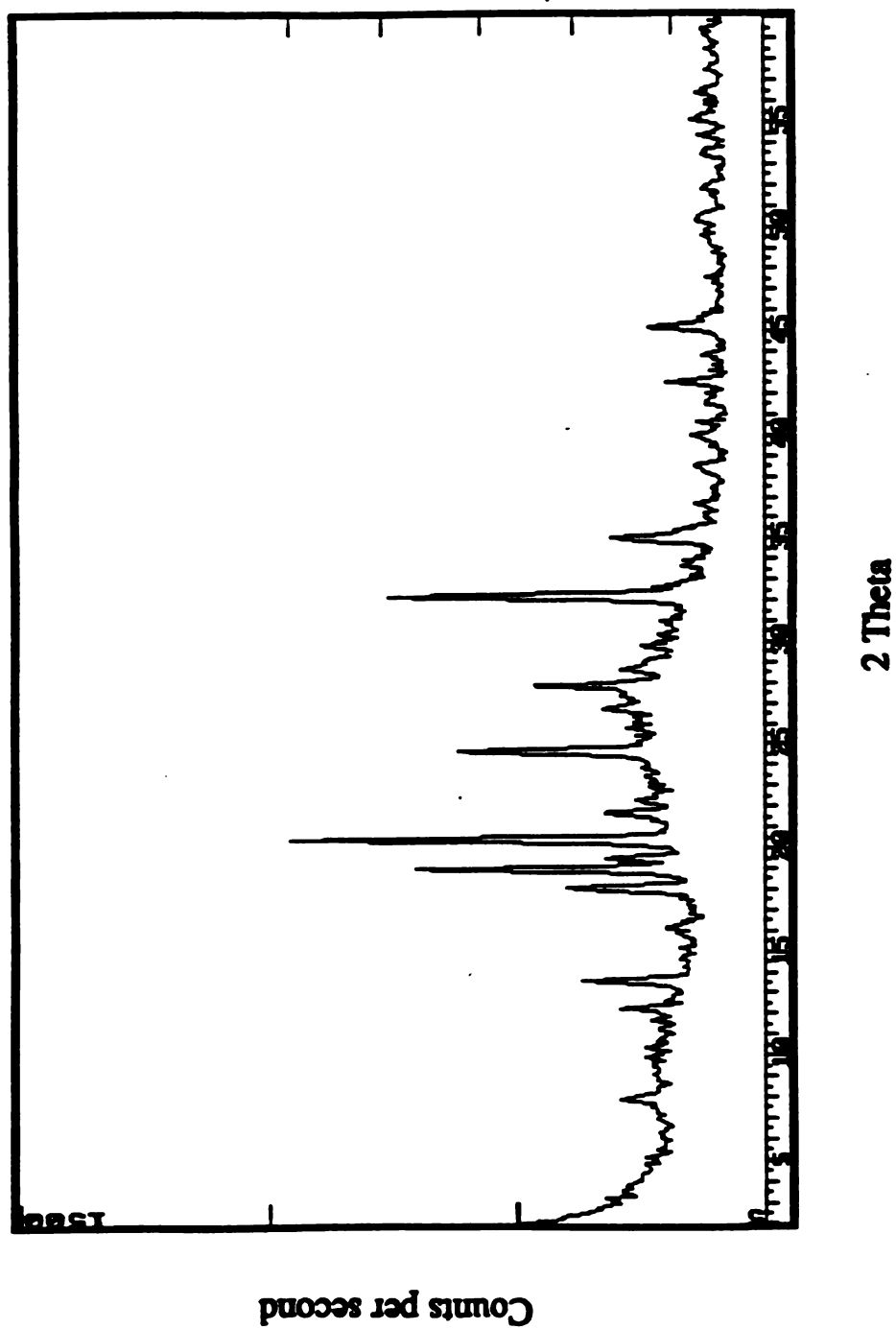
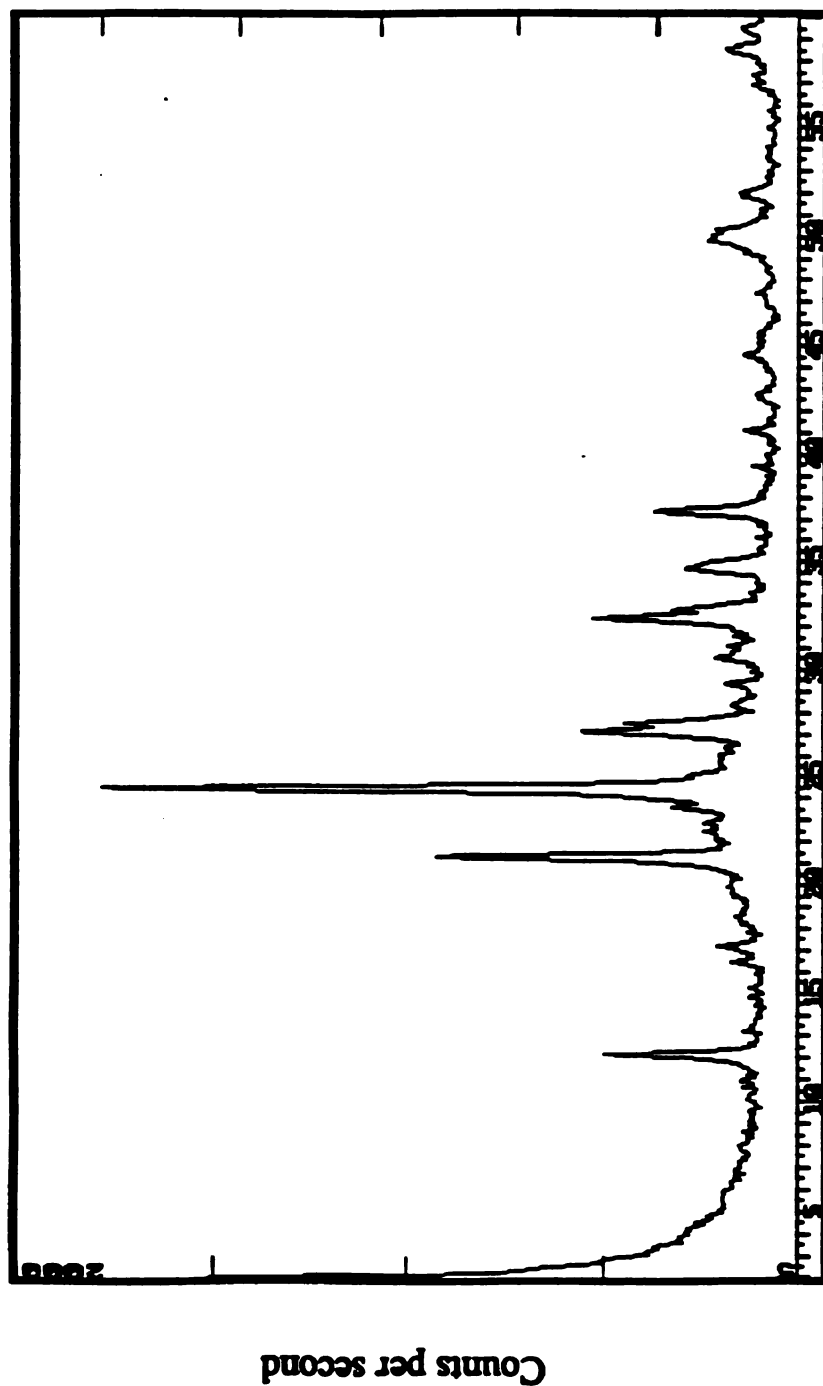
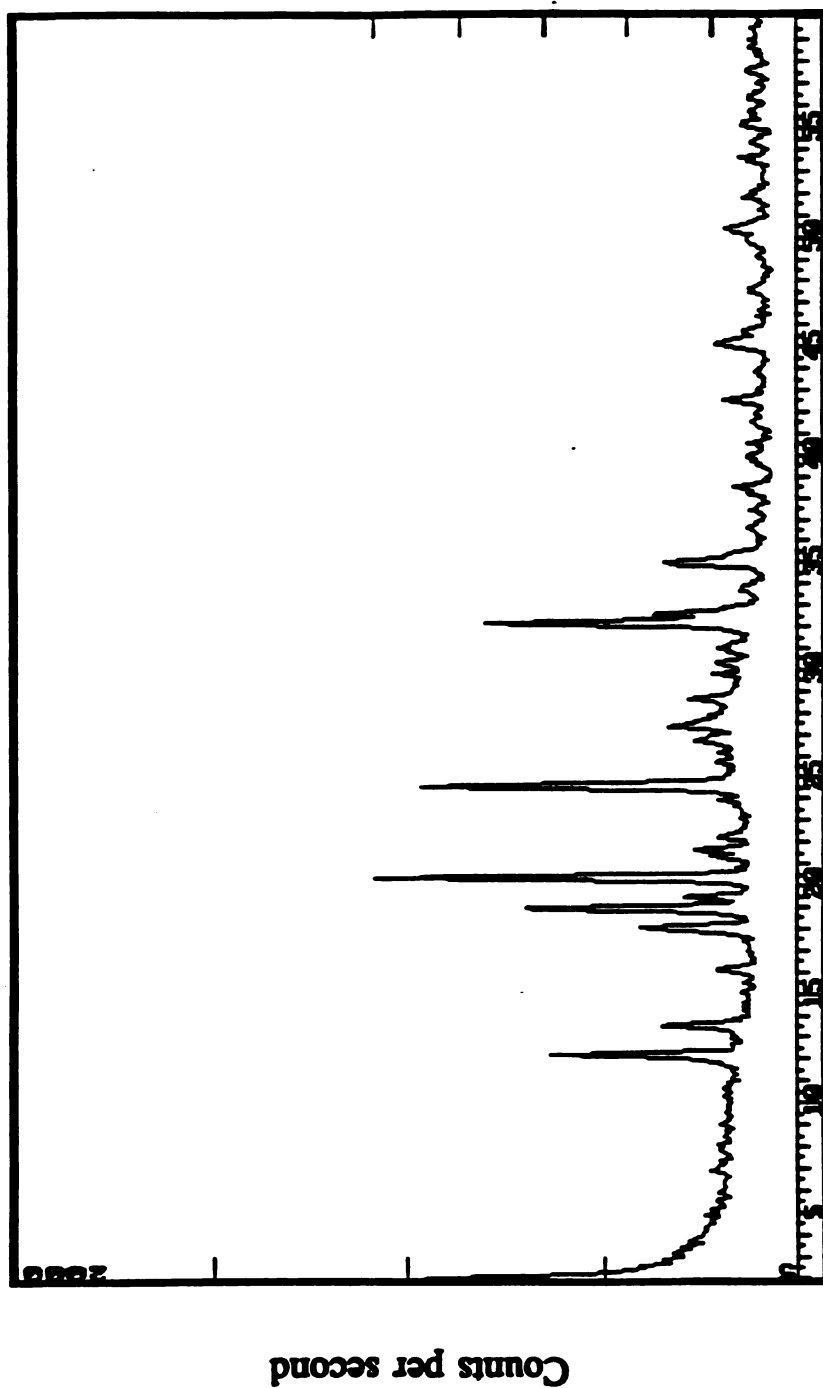


**Figure B-1 X-Ray diffraction spectrum of an iron phosphate catalyst supported by LUDOX @ HS 40%;
calcined at 110 °C**



2 Theta

**Figure B-2 X-Ray diffraction spectrum of an iron phosphate catalyst supported by LUDOX ® HS 40%;
calcined at 500 °C**



2 Theta

Figure B-3 X-Ray diffraction spectrum of an iron phosphate catalyst promoted with cerium; calcined at 110 °C

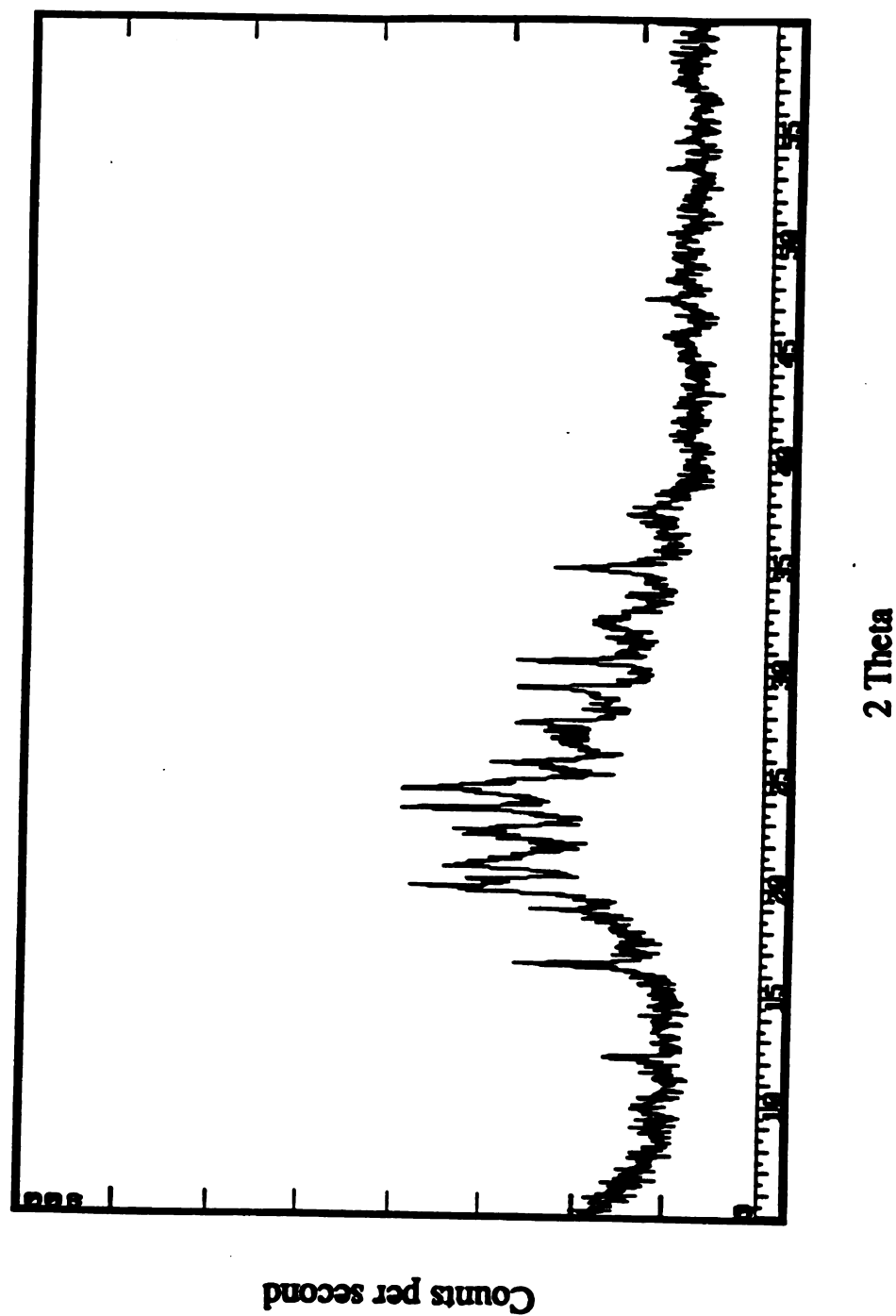
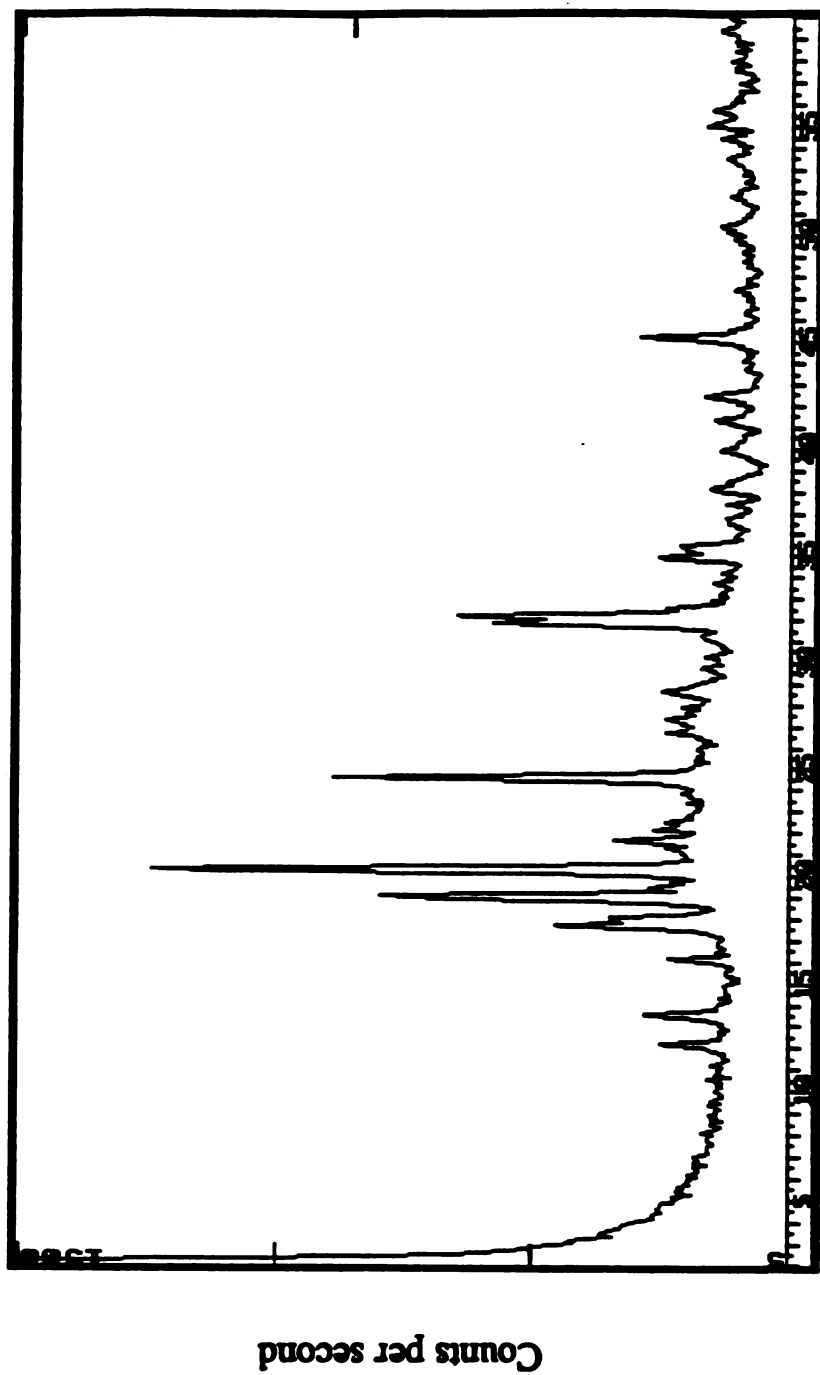
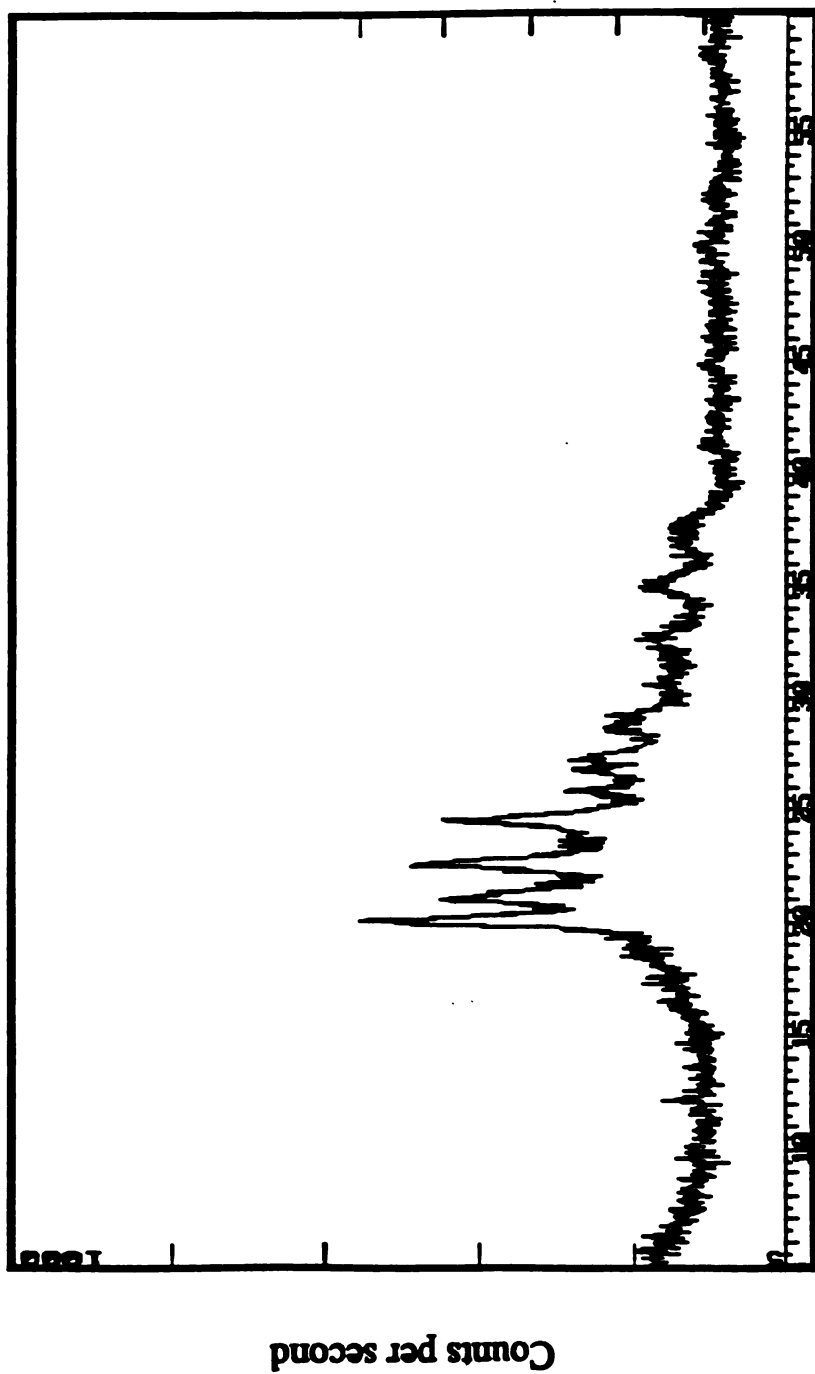


Figure B-4 X-Ray diffraction spectrum of an iron phosphate catalyst promoted with cerium; calcined at 500 °C



2 Theta

Figure B-5 X-Ray diffraction spectrum of an iron phosphate catalyst supported by LUDOX ® HS 40% and promoted with cerium; calcined at 110 °C



2 Theta

Figure B-6 X-Ray diffraction spectrum of an iron phosphate catalyst supported by LUDOX ® HS 40% and promoted with cerium; calcined at 500 °C

LIST OF REFERENCES

LIST OF REFERENCES

Bertolacini, R.J. (1989). Mechanical and Physical Testing of Catalysts. *Characterization and Catalyst Development- An Interactive Approach*. (Bradley, S.A., M.J.Gattuso, and R.J.Bertolacini, Eds.), p. 380, ACS Symposium Series 411, Washington D.C.

Bradley, S.A., E.Pitzer, and W.J.Koves. (1989). Bulk Crush Testing of Catalysts. *Characterization and Catalyst Development- An Interactive Approach*. (Bradley, S.A., M.J.Gattuso, and R.J.Bertolacini, Eds.), p. 398, ACS Symposium Series 411, Washington D.C.

Cohen, J.B. (1990). X-ray Diffraction Studies of Catalysts. *Ultramicroscopy*, 34: 41-46.

Cooley, S.D. and J.D.Powers. (1983). Maleic Acid and Anhydride. *Encyclopaedia of Chemical Processing and Design*, Vol. 29 (McKetta J.J., and W.A.Cunningham Eds.), p. 35-55, Marcel Dekker Inc., New York.

Cullity, B.D. (1956). *Elements of X-Ray Diffraction*, Addison-Wesley, Reading, Massachusetts.

Daniel, C. (1982). Oxydehydrogenation Process for Preparing Methacrylic acid and its Lower Alkyl Esters. *U.S.Patent 4,355,176*.

Daniel, C. (1983b). Oxydehydrogenation of Isobutyric acid and its Lower Alkyl Esters. *U.S.Patent 4,391,989*.

Daniel, C. (1983c). Oxydehydrogenation Process. *U.S.Patent 4,410,723*.

Daniel, C. (1983d). Oxydehydrogenation Process for Preparing Methacrylic acid and its Lower Alkyl Esters. *U.S.Patent 4,410,729*.

Daniel, C. (1983e). Oxydehydrogenation Process. *U.S.Patent 4,410,728*.

Daniel, C. (1984). Oxydehydrogenation Process. *U.S.Patent 4,439,621*.

Daniel, C., and P.L.Brusky. (1981b). Catalytic Oxydehydrogenation Process. *U.S.Patent 4,299,980*.

Daniel, C., and P.L.Brusky. (1983a). Catalytic Oxydehydrogenation Process. *U.S.Patent 4,374,268*.

Daniel, C., and P.L.Bursky. (1981a). Catalytic Oxydehydrogenation Process. *U.S.Patent 4,298,755*.

Delannay, F. (1984). Transmission Electron Microscopy and Related Microanalytical Techniques. *Characterization of Heterogeneous Catalysts*. (Delannay, F., Ed.), p. 71, Marcel Dekker, New York.

Delgass, W.N., G.Haller, R.Kellerman, and J.H.Lunsford. (1979). *Spectroscopy in Heterogeneous Catalysis*, Academic Press, New York.

Edmonds, T. (1980). The Characterization of Industrial Catalysts with ESCA. *Characterization of Catalysts*. (Thomas, J.M., and R.M.Lambert, Eds.), p. 30, John Wiley and Sons.

Haensel, V., and H.S.Haensel. (1989). The role of Catalyst Characterization in Process Development. *Characterization and Catalyst Development- An Interactive Approach*. (Bradley, S.A., M.J.Gattuso, and R.J.Bertolacini, Eds.), p. 2, ACS Symposium Series 411, Washington D.C.

Hightower, J.W. (1990). Kinetics and Mechanism. Lecture notes from 'Applications of Heterogeneous Catalysis', University of Houston, Houston, TX. December 3-7, 1990. p. C-34.

Howie, A. (1980). The Study of Supported Catalysts by Transmission Electron Microscopy. *Characterization of Catalysts*. (Thomas, J.M., and R.M.Lambert, Eds.), p. 12, John Wiley and Sons.

Irving-Monshaw, S., and A.Kislin. (1989). Lively Markets Brighten Maleic Anhydride Horizons. *Chemical Engineering*, 96(3): 35.

Jacobs, P.A. (1984). The Measurement of Surface Acidity. *Characterization of Heterogeneous Catalysts*. (Delannay, F., Ed.), p. 367, Marcel Dekker, New York.

Jones, W. (1980). Use of Mössbauer Spectroscopy for Catalyst Characterization. *Characterization of Catalysts*. (Thomas, J.M., and R.M.Lambert, Eds.), p. 114, John Wiley and Sons.

Kenney, C.N. (1980). Concluding Remarks - Comments by a Chemical Engineer. *Characterization of Catalysts*. (Thomas, J.M., and R.M.Lambert, Eds.), p. 274, John Wiley and Sons.

Lecloux, A.J. (1981). Texture of Catalysts. *Catalysis, Science and Technology, Vol. 2* (Anderson, J.R., and M.Boudart, Eds.), p. 171, Springer-Verlag, New York.

Lemaitre, J.L. (1984). Temperature Programmed Methods. *Characterization of Heterogeneous Catalysts*. (Delannay, F., Ed.), p. 29, Marcel Dekker, New York.

Lemaitre, J.L., P.Govind Menon, and F.Delannay. (1984). The Measurement of Catalyst Dispersion. *Characterization of Heterogeneous Catalysts*. (Delannay, F., Ed.), p. 299, Marcel Dekker, New York.

McCarvey, G.B., and J.B.Moffat. (1991). The Oxidative Dehydrogenation of Isobutyric acid to Methacrylic acid on Ion Exchange Modified 12-Heteropoly Oxometalates. *Journal of Catalysis*, 132: 100-116.

Millet, J.M., C.Virely, M.Forissier, P.Bussiere, and J.C.Vedrine. (1989). Mössbauer Spectroscopic Study of Iron Phosphate Catalysts used in Selective Oxidation. *Hyperfine Interactions*, 46: 619-628.

Millet, Jean-Marc M., and J.C.Vedrine. (1991). Role of Cesium in Iron Phosphates used in Isobutyric acid Oxidative Dehydrogenation. *Applied Catalysis*, 76: 209-219.

Millet, Jean-Marc M., J.C.Vedrine, and G. Hecquet. (1990). Proposal for Active Sites of Iron Phosphates in Isobutyric Oxidative Dehydrogenation Reaction. *New Developments in Selective Oxidation*. (Centi, G. and F.Trifiro, Eds.) Elsevier Science Publishers B.V., Amsterdam, p. 833-840.

Müller-Erlwein, E., and H.Hofmann. (1988). Determination of Kinetic Parameters from Dynamic Investigations of Heterogeneously Catalyzed Reactions. *Chemical Engineering Science*, 43(8): 2245-2250.

Pedersen S.E., N.J.Bremer, and J.L.Callahan. (1984). Iron - Phosphorus Mixed Oxide Catalysts and Process for their Preparation. *U.S.Patent 4,427,792*.

Richardson, J.T. (1989). *Principles of Catalyst Development*. Plenum Press, New York.

Robinson, W.D., and R.A.Mount. (1983). Maleic Anhydride, Maleic and Fumaric Acid. *Kirk-Othmer Encyclopaedia of Chemical Technology*, Vol. 14 (Mark et al., Eds.), John Wiley & Sons, p. 770-793.

Ruszala, F.A. (1983b). Oxydehydrogenation of Isobutyric acid and its Lower Alkyl Esters. *U.S.Patent 4,391,990*.

Ruszala, F.A. (1984). Oxydehydrogenation of Isobutyric acid and its Lower Alkyl Esters. *U.S.Patent 4,434,298*.

Ruszala, F.A., and T.J.Weeks. (1983a). Oxydehydrogenation Process for Preparing Methacrylic acid and its Lower Alkyl Esters. *U.S.Patent 4,374,270*.

Seamans, J.D., J.G.Welch, and C.A.Vuitel. (1989). Improved Regeneration Quality with Length and Density Grading. *Characterization and Catalyst Development- An Interactive Approach*. (Bradley, S.A., M.J.Gattuso, and R.J.Bertolacini, Eds.), p. 2, ACS Symposium Series 411, Washington D.C.

Sing, K.S.W. (1980). The Use of Physisorption for the Determination of Surface Area and Pore Size Distribution. *Characterization of Catalysts*. (Thomas, J.M., and R.M.Lambert, Eds.), p. 12, John Wiley and Sons.

Statz, R.J., and J.K.Doty. (1980). Catalyst and Dehydrogenation Process. *U.S.Patent 4,232,174*.

Szmant, H.H. (1989). *Organic Building Blocks of the Chemical Industry*. John Wiley and Sons. p. 312.

Watkins, W.C. (1974). Catalytic Process for the Manufacture of Unsaturated Acids and Esters. *U.S. Patent 3,855,279*.

Watkins, W.C. (1975). Catalytic Process for the Manufacture of Unsaturated Acids and Esters. *U.S. Patent 3,917,673*.

Watzenberger, O., G. Emig, and D.T.Lynch. (1990). Oxydehydrogenation of Isobutyric acid with Heteropolyacid Catalysts: Experimental Observations of Deactivation. *Journal of Catalysis*, 124: 247-258.

Wood, Andrew. (1990). Maleic Anhydride's Growing Pains. *Chemical Week*, 146(16): 6.

MICHIGAN STATE UNIV. LIBRARIES



31293010559767